DOSE OPTIMISATION IN CONTEMPORARY DIGITAL LATERAL CEPHALOMETRY

BY

RAHUL KHIROYA

BDS MJDFRCS

A THESIS SUBMITTED TO THE FACULTY OF MEDICINE AND DENTISTRY OF THE UNIVERSITY OF BIRMINGHAM FOR THE DEGREE OF

MASTER OF PHILOSOPHY

DEPARTMENT OF ORTHODONTICS

THE DENTAL SCHOOL

ST CHAD'S QUEENSWAY

BIRMINGHAM

B4 6NN

OCTOBER 2012

ABSTRACT

AIM

To investigate whether health risk may be reduced in a patient population when taking a lateral cephalogram.

METHOD

A laboratory study to determine the minimum effective radiation dose required to obtain a digital lateral cephalogram capable of being analysed by an on-screen method within an acceptable degree of clinical error.

To survey hospital based orthodontic departments in the West Midlands and use the gathered information to estimate what effective dose patients are being exposed to from lateral cephalometric exposures.

RESULTS

Using the mean of each of the 10 recruited clinicians' cephalometric measurements with 95% confidence intervals for the mean defined, clinically significant error appears not to have affected cephalometric measurements taken from any of the seven lateral cephalograms analysed down to a minimum effective radiation dose of 0.06μSv.

The results of the hospital survey indicate units are exposing patients to an effective radiation dose of between 0.5μSv-2.4μSv.

CONCLUSIONS

A reduction in effective radiation dose and health risk may be possible to patients within the West Midlands during routine lateral cephalometric exposures.

ACKNOWLEDGEMENTS

I gratefully acknowledge and thank my clinical supervisor Mr Peter Rice for the inspirational idea and backing behind this research. Professor Damien Walmsley for his academic supervision and enthusiastic help with the writing up of the thesis. Dr Sayeed Haque for his statistical expertise. Elizabeth Larkin and her colleagues for their support with the acquisition of lateral cephalograms, dosimetry and radiation-physics expertise. The radiographers at the Birmingham Dental Hospital. CIRS (Norfolk, VA, USA) for their lease of the tissue-equivalent phantom used for this study.

I also thank my devoted wife Sheetal and the Khiroya family for their encouragement through what has been one of my most challenging endeavours to date.

CONTENTS

FIGURES

TABLES

INTRODUCTION

In order to produce a lateral cephalogram, orthodontic patients are exposed to X-rays, which are an ionising type of radiation. The risk associated is for a potential somatic stochastic effect, which is the possibility of inducing a cancer in the directly irradiated radiosensitive organs within the head and neck (Forsyth et al. 1996).

Orthodontic patients are typically at the stage of early adolescence and actively growing they are therefore potentially more susceptible than adults to potential somatic stochastic effects.

When taking a lateral cephalogram effective radiation dose has been found to vary depending on the X-ray equipment used. Published literature would indicate that typical effective dose expected from a lateral cephalogram is approximately 3μSv and that the risk of inducing a malignancy following such an exposure is less than one patient per million (Isaacson et al., 2008).

Although the radiographic exposure and potential risk may be perceived to be small any reduction in radiographic exposure to the patient from lateral cephalometric radiographs would be of benefit due to the cumulative dose risk associated with any type of ionising radiation (Forsyth et al., 1996). The aim of radiation protection is to ensure radiographic exposures are justified and radiation dose is kept as low as reasonably practicable 'ALARP' (Health and Safety Executive).

Any study to attempt to reduce effective radiation dose in lateral cephalometry would be of obvious benefit. Such studies also address public concern regards over-exposure to radiation during radiographic procedures. A recent article published in the Independent Newspaper voiced the following concern “patients are being exposed to unnecessarily high dose of radiation during common X-rays and scans because some hospitals have out-of-date equipment and inadequately trained staff” (Lakhani, 2010).

LITERATURE REVIEW

1. LATERAL CEPHALOMETRY AND ORTHODONTICS

A scientific approach to the investigation of the human craniofacial pattern was first undertaken by anthropologists and anatomists who recorded the various dimensions of ancient dry skulls from defined osteological landmarks. The principles of the measurement technique used on dry skulls were later applied to living subjects and the measurement of the head of a living subject from defined osteological landmarks came to be known as 'craniometry'. Unlike on dry skulls the osteological landmarks of interest had to be located by palpation through supra-adjacent soft tissue. This primitive method without any form of visualization of the osteological landmarks meant craniometry remained subjective.

The discovery of X-rays by Roentgen in 1895 revolutionised craniometry. A radiographic head image could be taken allowing osteological landmarks to be visualised on a film. This new method of identification of osteological landmarks in two dimensions allowed for a much more accurate method of studying human craniofacial pattern.

Scientists recognised that a correctly standardised radiographic technique had the potential to allow demonstration of facial and dento-skeletal relationships along with illustrating how the cranial base, jaws and teeth relate to one another. Such a

technique would also allow the accurate study of craniofacial growth and development.

In 1931 this vision became a reality, Broadbent in the United States of America and Hofrath in Germany almost simultaneously presented a standardised radiographic technique using an X-ray machine and a head holder called a cephalostat or cephalometer (Broadbent, 1931, Hofrath, 1931). This standardised radiographic technique allowed comparison of the radiographs of one patient taken on different occasions, or those of different individuals. This new standardised radiographic technique came to be known as cephalometry and the images taken using this method cephalograms. Over time the radiographic equipment used in cephalometry has advanced greatly but the standardised technique incorporating the use of a cephalostat has largely remained the same.

The use and application of cephalometry in orthodontics is an adjunct to a systematic clinical examination. As part of a clinical examination ethnic background, skeletal, dental and physiological age, overlying facial soft tissue form and the function of the teeth are recorded. Cephalometric radiographs are routinely indicated to aid diagnosis and help to confirm any underlying skeletal or soft tissue abnormalities. Such findings most commonly assist in the process of orthodontic treatment planning. During the course of a patient's treatment subsequent cephalometric radiographs maybe indicated to allow the clinician to monitor treatment progress or even assist treatment planning a second phase of orthodontic treatment. A cephalometric radiograph may also be required to appraise treatment

results before the completion of active treatment to ensure that treatment targets have been met and to allow planning of orthodontic retention. Cephalometric radiographs are also used in research to study growth and the effects of different treatment protocols.

2. ACQUISITION OF A LATERAL CEPHALOGRAM

The basic components for producing a lateral cephalogram are an X-ray apparatus, an image receptor and a cephalostat.

2.1 X-RAY APPARATUS

The X-ray apparatus is responsible for producing X-ray photons, a type of electromagnetic radiation in the form of a beam.

Typically the X-ray apparatus comprises an X-ray tube, transformers, filters, collimators and a coolant system. These components are all encased in the machine housing. The X-ray tube is at the heart of this apparatus and is essentially a high vacuum tube that serves as a source of X-ray photons. The three basic elements within the tube are a cathode, an anode and an electrical power supply.

Typically the cathode is a tungsten filament surrounded by a molybdenum-focusing cup. The anode comprises a small tungsten block embedded in a copper stem.

The tungsten filament serves as a source of electrons and is connected to allow a separate low and high voltage circuit. A step-down transformer supplies the low-voltage circuit with 10V and a high current to heat the tungsten filament until electrons are emitted. The production of electrons forms a cloud otherwise known as thermionic emission. A step-up transformer supplies the high-voltage circuit to typically create 60-90 kV. The potential difference between the cathode and the

anode accelerates the electron cloud, which forms electron beams. These are directed by the focusing cup to strike a small target on the anode called the focal spot. There is a release of kinetic energy as this occurs and this creates X-ray photons.

The importance of a coolant system in an X-ray apparatus cannot be understated. Interestingly it is only 1% of the energy that is converted to X-ray photons with the other 99% being lost as heat. Although tungsten is a high atomic weight substance necessary for producing X-ray photons, its thermal resistance is unable to withstand the heat that is generated during the process. Consequently, the copper stem acts as a thermal conductor, which dissipates the heat into an oil reservoir surrounding the X-ray tube.

Figure 1 Depiction of an X-ray tube and the production of X-ray photons (Ahlqvist et al., 1986)

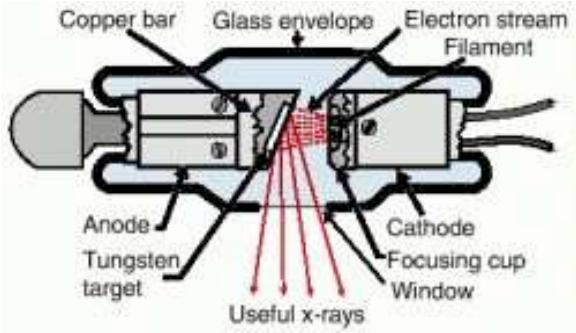

The size of the focal spot, which determines the image quality, follows the Benson Line Focus principle. This states '*the projection of the focal spot perpendicular to the*

electron beam (the effective focal spot) is smaller that the actual focal spot that projects perpendicular to the target'. Therefore, the target face in the X-ray tube is orientated at an angle of 15-20 degrees to the cathode. This allows a small focal spot to be created that increases the image sharpness. It also increases the heat capacity of the target. The focal spot created by the inclined target is generally between $1mm^2$ and $2mm^2$.

The X-ray photons that emerge from the target are made up of a divergent beam with differing energy levels. The low-energy (long wavelength) photons are filtered out by an aluminum filter. The divergent X-ray beam then passes through a lead diaphragm (the collimator) that fits over the opening of the machine housing. The collimator determines the size and shape of the beam. The setup is designed to allow only those X-ray photons with sufficient penetrating power to reach the patient.

2.2 THE IMAGE RECEPTOR SYSTEM

An image receptor system records the final picture produced by X-ray beam after it has passed through the subject.

There are three main types of image receptor systems used for cephalometry; film and screen, high density line scan solid state detectors and integrated flat panel detectors.

2.2.1 FILM AND SCREEN

Film and screen is the oldest system. It comprises the extra-oral film, which is either 8 inches by 10 inches (203mmx254mm) or 10 inches x 12 inches (254mmx305mm). It is a screened film that is sensitive to the fluorescent light radiated from an intensifying screen.

Basic components of an X-ray film are an emulsion of silver halide crystals suspended in a gelatin framework. A transparent blue tinted cellulose acetate serves as the base. When the silver halide crystals are exposed to the X-ray beam, they are converted to metallic silver deposited in the film, thereby producing a latent image. This is converted into a visible and permanent image after film processing. The amount of metallic silver deposited in the emulsion determines film density, whereas the grain size of the silver halide determines film sensitivity and definition.

Intensifying screens are used in pairs with a screened film to reduce the patient's exposure dose and increase image contrast by intensifying the photographic effect of the irradiation. Intensifying screens consist of phosphorescent crystals: Such as calcium tungstate and barium lead sulphate, coated onto a plastic support. When the crystals are exposed to an X-ray beam, they emit fluorescent light that is recorded by the film. The brightness of the light is directly related both to the intensity of the X-rays and to the size and quality of the phosphorescent crystals.

2.2.2 HIGH DENSITY LINE SCAN SOLID STATE DETECTORS

The use of high density line scan solid state detectors commonly known as memory phosphor plates have bridged the progression from film-based to direct digital imaging methods. An advantage of this type of image receptor is that it has the ability to fit within any pre-existing equipment designed for film-screen based technology without modification because it replaces just the existing film. This means a clinician can convert to using digital cephalometry without having to undergo the inconvenience and cost of replacing a whole X-ray apparatus.

Typically such an image receptor is composed of a photostimulable barium fluoro-bromide doped with europium (BaFlBr:Eu) or cesium bromide (CsBr) phosphor.

After an exposure, excited electrons in the material within the detector plate remain 'trapped' in 'colour centres' in the crystal lattice until stimulated by a second illumination. This phenomenon is known as photostimulable luminescence. The exposed detector plate is placed in a scanner (connected to a computer and display) where the latent formed image is retrieved point-by-point and digitised, using laser light scanning. An image data file is produced which can be displayed on a computer.

Using a memory phosphor plate the scanning process replaces the chemical development process as compared to a film based image receptor. As a result it is not much faster than film processing however unlike film a memory phosphor plate can be reused by exposing the plate to room intensity white light to “erase it”.

2.2.3 INTEGRATED FLAT PANEL DETECTORS

The most recent innovation in image receptor design are the integrated flat panel detectors which can be split into the two categories of integrated indirect and direct flat panel detectors.

Indirect flat panel detectors are typically composed of amorphous silicon (a-Si). They combine amorphous silicon detectors with a scintillator in the detector's outer layer made from Caesium Iodide (CsI), or Gadolinium Oxysulfide (Gd_2O_2S).

It is due to the conversion of X-ray energy to light by the scintillator that this type of detector is considered an indirect image capture technology. The converted light is channelled through the amorphous silicon photodiode layer of the amorphous silicon and is converted to a digital output signal. The signal is translated by Thin Film Transistors (TFTs) or by fibre coupled Charged Couple Devices (CCDs) to an image data file which can be viewed on a computer.

Direct flat panel detectors are typically composed of amorphous selenium (a-Se). In comparison to their indirect counterpart, the X-ray photons which reach this type of detector are converted directly to charge. A TFT array, active matrix array, electrometer probes or microplasma line addressing reads out the resultant charge pattern in the selenium layer of the detector producing an image data file which can be viewed on a computer.

An integrated flat panel detector is exposed to the X-ray beam differently as compared to X-ray film or a memory phosphor plate.

With use of X-ray film or a memory phosphor plate the whole skull is pictured simultaneously with a pyramid-shaped X-ray beam. The typical total exposure time for these types of image receptor is approximately 0.5 seconds.

Typically when an integrated flat panel detector system is used the X-ray apparatus works using a narrow beam linear scanning process called a “slot technique”. The patient’s head is scanned in linear slices with a flat fan shaped X-ray beam. During the scanning process, which takes about 15.8 seconds, the patient must stay motionless. From the total height of the scanned distance (210mm) and the height of the fan-shaped X-ray beam in the plane of the sensor (3.6mm) the ratio of the total to the effective exposure time can be calculated: 210/3.6=58.3. Therefore a time of 15.8 seconds for acquisition of the digital image yields an effective exposure time in each part of the skull of (15.8/58.3)=0.27 seconds. The “slot technique” compared to a pyramid shaped X-ray beam is illustrated in Figure 2.

Figure 2 The “slot technique” (b) compared to (a) the conventional pyramid-shaped X-ray beam (Visser et al., 2001).

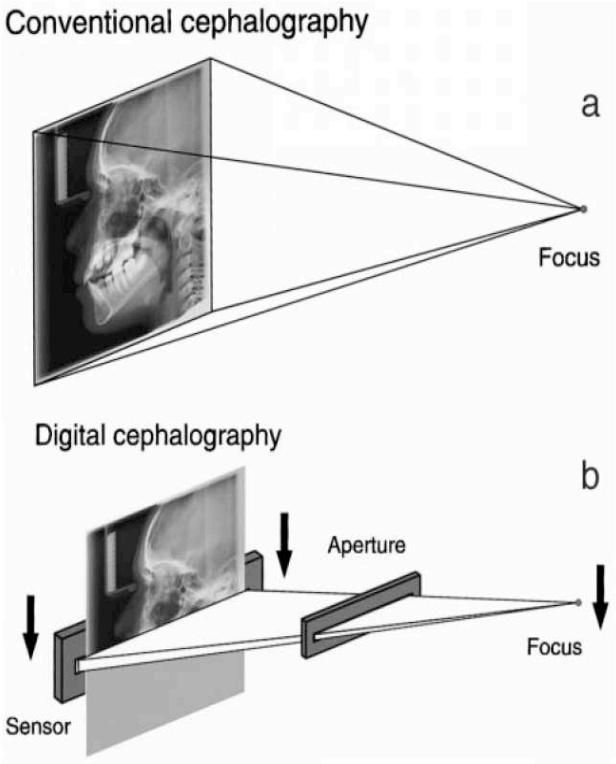

2.3 THE CEPHALOSTAT AND PATIENT POSITIONING

The use of a cephalostat, also termed a head-holder or cephalometer, is used to help standardize the technique of cephalometry. The patient’s head is fixed by an ear-rod that is inserted into each external auditory meatus. The upper border of the auditory meatus rests on the upper part of the ear-rod. The head is centered in the cephalostat and is orientated in natural head position with the Frankfort plane parallel to the floor and the mid-sagittal plane both vertical and parallel to the image

receptor. The upper part of the face is supported by a forehead clamp, positioned at nasion.

The patient's head should be in a constant fixed position during the entire exposure. The ear-rods should allow for small adjustments of the head to correct undesirable lateral tilt or rotation (Solow and Kreiborg, 1988).

The subject's teeth should be in centric occlusion and the lips in repose, unless other specifications have been recommended (e.g. with the mouth open or with a specific inter-occlusal registration used as orientation).

The focus-image receptor distance is usually around 5 feet (152.4cm). It is convention for the left side of the head to face the image receptor. This is because the left side is less prone to distortion than the right side of the head, which is further from the image receptor. Skin markers are sometimes used to aid identification of points on the left side of the head.

3. CEPHALOMETRIC ANALYSIS

The technique of taking linear and angular measurements from defined cephalometric landmarks (previously described as osteological landmarks) of a cephalogram and analysing them is known as a cephalometric analysis. In practice these cephalometric landmarks are identified from a cephalogram and traditionally transferred from the X-ray film to an overlying sheet of tracing paper or acetate. More recently digital recording is being used particularly with the advent of digital cephalometry (Figure 3). This more contemporary technique has been demonstrated to allow clinically accurate landmark identification and measurements to be made (Chen et al., 2004, McClure et al., 2005, Ongkosuwito et al., 2002).

Cephalometric landmarks used for cephalometric analysis have been described as the "*extrema of a tissue component with respect to a spatial component*" (Rudolph et al., 1998). Landmarks common to a number of analyses have been adopted due to their ease of reproducibility. Some of the more commonly used cephalometric landmarks and their definitions have been listed in Table 1 and illustrated in Figure 4.

Common cephalometric planes and angles, which are constructed from the cephalometric landmarks, are defined in Tables 2 and 3 and illustrated in Figures 5 and 6. It should be noted that these can vary according to the type of analysis being undertaken.

For all angles and measurements specific to an analysis there are a set of racially derived normal values. Normal 'Eastman Analysis' values for a Caucasian patient have been illustrated in Table 4. The numbers in brackets next to the normal values represent one standard deviation above or below the set normal value within which an angle or measurement would be deemed to still be within normal limits. These measurements allow the clinician to gauge the size and spatial relationships of the teeth, jaw and cranium and identify how closely they match to a set of racially derived norms. In providing information like this cephalometric analysis can therefore inform treatment planning, quantify changes during treatment and provide data for clinical research.

Serial cephalometric radiographs taken prior, during and after treatment enable monitoring of treatment progress through superimposition of radiographic images over stable anatomical features. Differences in cephalometric measurements are attributable to the effects of treatment and naturally occurring growth.

Figure 3 An image of a digitised cephalometric tracing superimposed over a digital cephalogram

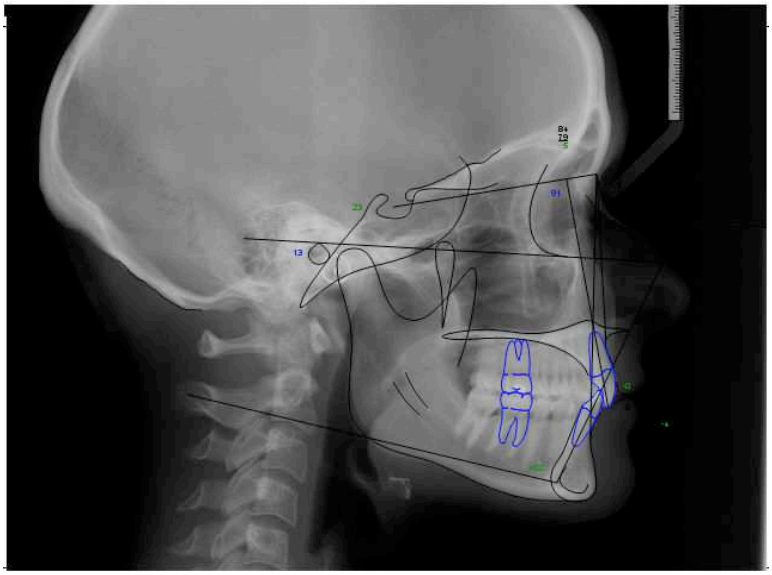

Table 1 Cephalometric Landmarks and descriptions of their anatomical location (Whaites, 2006)

Cephalometric Landmark	Anatomical Location
Sella (S)	The centre of the Sella Turnica (determined by inspection)
Orbitale (Or)	The lowest point on the infra-orbital margin
Nasion (N)	The most anterior point on the frontonasal suture
Anterior Nasal Spine (ANS)	The tip of the anterior nasal spine
Subspinale or point A	The deepest midline point between the anterior nasal spine and Prosthion
Prosthion (Pr)	The most anterior point of the alveolar crest in the premaxilla, usually between the upper central incisors
Infradentale (Id)	The most anterior point of the alveolar crest, situated between the lower central incisors.
Supramentale or point B	The deepest point in the bony outline between the Infradentale and Pogonion
Pogonion (Pog)	The most anterior point of the bony chin
Gnathion (Gn)	The most anterior and inferior point on the bony outline of the chin, situated equidistant from Pogonion and Menton
Menton (Me)	The lowest point on the bony outline of the mandibular symphysis
Gonion (Go)	The most lateral external point at the junction of the horizontal and ascending rami of the mandible
Posterior Nasal Spine (PNS)	The tip of the posterior spine of the palatine bone in the hard palate
Articulare (Ar)	The point of intersection of the dorsal contours of the posterior border of the mandible and temporal bone
Porion (Po)	The uppermost point of the bony external auditory meatus, usually regarded as coincidental with the uppermost point of the ear rods of the cephalostat

Figure 4 Diagrammatic representation of main cephalometric landmarks (Whaites, 2006)

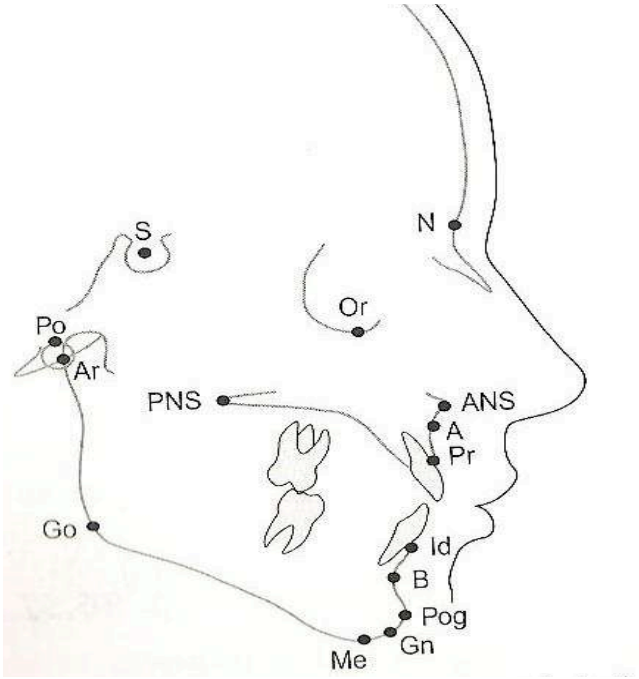

Figure 5 Diagrammatic representation of cephalometric planes (Whaites, 2006)

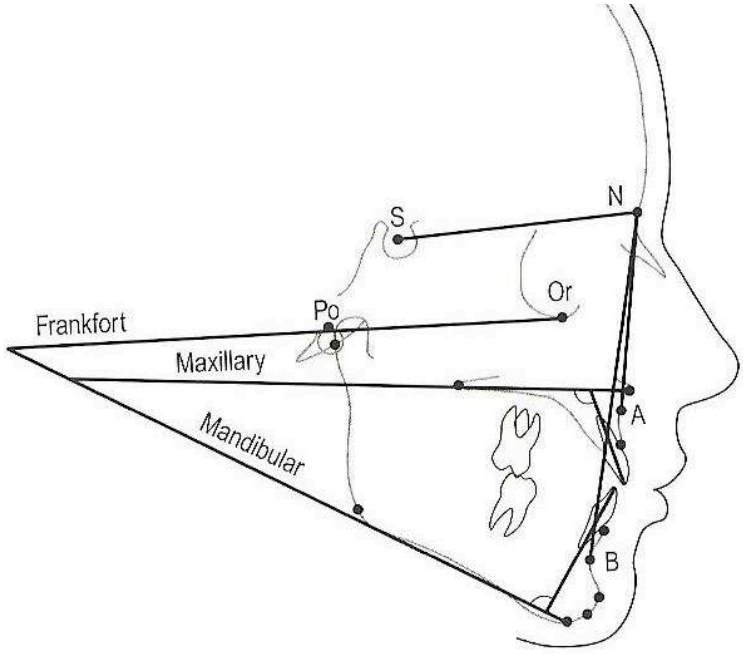

Table 2 Cephalometric Planes (Whaites, 2006)

Cephalometric Plane	Description
Frankfort Plane	A transverse plane through the skull represented by the line joining Porion and Orbitale.
Mandibular Plane	A transverse plane through the skull representing the lower border of the horizontal ramus of the mandible. There are several definitions: • A tangent to the lower border of the mandible • A line joining Gnathion and Gonion • A line joining Menton and Gonion
Maxillary Plane	A transverse plane through the skull represented by the line joining Sella and Nasion
SN Plane	A transverse plane through the skull represented by the line joining Sella and Nasion

Table 3 Cephalometric Angles (Whaites, 2006)

Cephalometric Angle	Description
SNA	Relates the anteroposterior position of the maxilla, as represented by the A point, to the cranial base.
SNB	Relates the anteroposterior position of the mandible, as represented by the B point, to the cranial base
ANB	Relates the anteroposterior position of the maxilla to the mandible i.e. indicates the anteroposterior skeletal pattern – Class I, II or III.
Upper Incisal Proclination	The angle between the long axis of the maxillary incisors and the maxillary plane.
Lower incisal inclination	The angle between the long axis of the mandibular incisors and the mandibular plane.

Table 4 Normal 'Eastman Analysis' values for a Caucasian patient (Gill, 2008)

Measurement	Normal Angulation in degrees (Standard Deviation)
SNA	81 (3)
SNB	78 (3)
ANB	3 (2)
MMPA	27 (4)
Upper Incisal Proclination	109 (6)
Lower Incisal Proclination	93 (6)
Interincisal Angle	135 (10)

Figure 6 Diagrammatic representation of cephalometric angles (Gill, 2008)

Upper and Lower Incisal Proclination

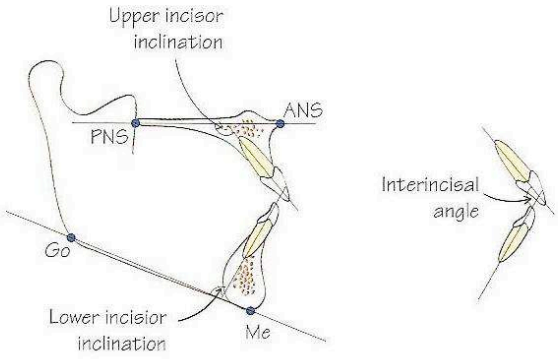

SNA, SNB and ANB

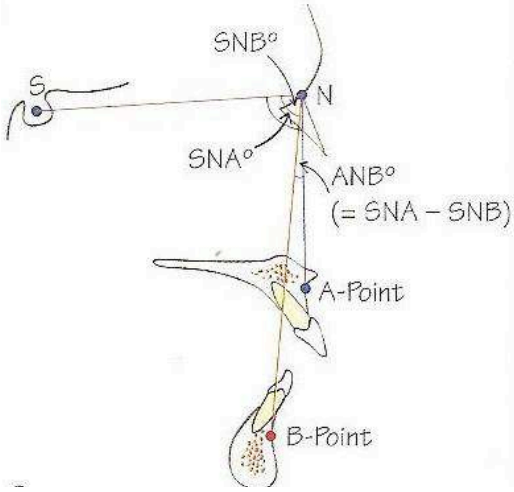

4. SOURCES OF ERROR IN CEPHALOMETRY

If one is to draw conclusions from cephalometric analysis, it is important that all sources of error are kept to a minimum, errors should be identified and corrections made where possible.

Errors in cephalometry can be introduced at the two main stages of the process, the first being initially when attaining the cephalogram and or later during the subsequent cephalometric analysis.

Errors in cephalometry fall into two main categories; systematic and random.

Systematic error implies a bias in the recording and measuring system (Cohen, 1984). It can arise from the geometric magnification of the radiographic image, or where the same radiograph is measured by two different individuals whose conceptual view of the landmark may be different. They are important in that they may exaggerate or obscure differences between variables.

Random errors can arise because of the uncertainty in identifying a landmark and therefore the clinician's decision concerning a landmark may vary at random. Poor positioning of the patient in the cephalostat or lack of resolution can prevent accurate identification. Random errors add to the natural variability of the measurements and may therefore hide real differences between groups.

Broadly speaking measurements based on radiographic images may be prone to error through: Radiographic projection errors, errors within the measuring system, errors in landmark identification (Athanasiou, 1995)

4.1 RADIOGRAPHIC PROJECTION ERRORS

Radiographic projection errors are caused by the projection of a three dimensional object onto a two-dimensional film which may result in unwanted magnification and shape distortion of the resulting image. These errors tend to be of little importance owing to their magnitude however they may be important where a subject has an actual skull asymmetry.

The degree of magnification will depend on the positioning of the focus, object and film (Hixon, 1960). It is suggested good practice that some form of scale is included in the radiographic image so that the degree of magnification can easily be identified. The percentage of magnification can be calculated using the following equation:

Magnification (%) = {focus-film distance/focus-film distance – object-film distance} -1 x 100

Shape distortion results in an image that does not correspond proportionally to the subject. In the case of a skull, which is a three-dimensional object, distortion usually occurs because of improper orientation of the patient's head in the cephalostat or improper alignment of the image receptor and central X-ray beam. Placing the image receptor parallel to the mid-sagittal plane of the head and projecting the X-ray beam

perpendicularly to the image receptor and the mid-sagittal plane can minimise this form of distortion. The lateral cephalogram can be further distorted by the foreshortening of distances between points lying in different planes and by the radial displacement of all points and structures that are not located in the centre of the X-ray beam.

The effects of poor patient positioning on linear measurements using a mathematical model have been studied. It has been reported that in general, projection errors in length measurements are minor in cephalometry (Ahlqvist et al., 1986). Head rotations of less than or equal to 5 degrees produce insignificant errors which in the majority of occasions would be hidden by other errors (landmark identification and registration). However a head rotation above 5 degrees may produce a more significant error. By ensuring that head position remains constant between radiographic episodes any changes should be as a result of growth and or treatment and not due to changes in orientation of head position.

4.2 ERRORS WITHIN THE MEASURING SYSTEM

Ultimately the measurement system can contribute to measurement error. Currently the trend in contemporary orthodontics is to use orthodontic software particularly with the advent of digital cephalometry. Traditional (hand-tracing) and computerised methods of cephalometric analysis have been compared, the difference between methods have been found to be insignificant (Chen et al., 2004, McClure et al., 2005, Ongkosuwito et al., 2002, Turner and Weerakone, 2001). More recently the

traditional method has been compared with a computerised method incorporating orthodontic software (Dolphin Imaging 9), where lateral cephalograms were scanned at 300 dpi and digitised onscreen (Sayinsu et al., 2007). The findings demonstrated that the use of computer software for cephalometric analysis carried out on scanned images did not increase the measurement error when compared with hand tracing.

4.3 ERRORS IN LANDMARK IDENTIFICATION

The process of landmark identification as a source of error has been widely commented upon. It is considered to be the major source of cephalometric error provided that the measuring system is used accurately (Baumrind and Frantz, 1971, Midtgard et al., 1974, Richardson, 1966). In a key investigation, patients underwent repeat lateral cephalograms for clinical purposes; the greater error variance was from the actual analyses whilst the error variance in repeating the radiographs proved to be small (Houston et al., 1986). The reliability of landmark identification is dependent on numerous factors which include: The general quality of the radiographic image, the operator and registration procedure, characteristics of the cranial structures, accuracy of landmark identification and reproducibility.

5. HEALTH AND SAFETY

5.1 IONISING RADIATION - EFFECTS AND ASSOCIATED RISKS

X-rays are an ionising type of electromagnetic radiation and therefore their benefits in radiography do not come without risk to the patient and potentially the staff taking the radiographs. X-rays can cause ionisation of the contents of living cells, which can lead to irreversible damage. The greatest concern is that damage to the DNA of a cell will occur. Interaction of X-rays may take place directly with the DNA or indirectly when an X-ray disrupts a water molecule into reactive radicals that go on to damage DNA.

Damage to the DNA of a cell can result in genetic or somatic effects. Somatic effects are those that occur in the irradiated somatic cells of an individual. Genetic effects are those that occur in the germ cells and are transmitted to the offspring of the irradiated individual.

Genetic effects are most likely to occur because of gonadal irradiation. During dental radiography, genetic effects are not usually considered because the gonads should not be in the path of the beam. Therefore the main concern is for somatic effects.

Somatic effects can be further split into deterministic and stochastic effects. All deterministic effects have threshold doses below which they do not occur (threshold doses for the main categories of deterministic effects are illustrated in Table 5 (NHS, 2007)). Above the threshold dose, the determinsitic effect is certain to occur; below

the threshold dose the effect should not occur. In dental radiography these thresholds should never be reached. In contrast the same cannot be said for stochastic effects i.e. tumour induction and therefore a clinician's main concern should be that however small the radiation exposure to the patient, there is always a risk of causing a stochastic effect such as a malignancy.

Table 5 Threshold doses for deterministic effects

Tissue	Effect	Threshold absorbed dose (Gy)
Testes	Temporary sterility Permanent sterility	~ 0.1 ~ 6
Ovaries	Sterility	~ 3
Lens of the eye	Cataract	~ 0.5
Bone marrow	Depression of haematopoiesis	~ 0.5
Skin	Reddening (erythema) Erythema & desquamation	<3 – 6 5 – 10

5.2 RADIOSENSITIVE ANATOMY OF THE HEAD AND NECK

There is a known carcinogenic risk to patients from any exposure to radiation, no matter how small and the risk factor is greater for children than adults. The cells in a child are much more sensitive to the carcinogenic actions of radiation (Lurie, 1981). The main reason for this is that the cells in a child are much more actively dividing than in adults. Children are also much more susceptible than adults due to being more likely to live a greater number of years to allow the effects of irradiation to

become apparent; the latency period for radiogenic cancer being approximately 20-35 years. (Lurie, 1981).

In cephalometry the main hazard is the chance of inducing cancers in the directly irradiated radiosensitive tissues within the head and neck (Forsyth et al., 1996). The radiosensitive tissues that are likely to be irradiated during cephalometry include the bone-marrow, lymphoid, thyroid, bone surface, brain, salivary glands and skin. The thyroid gland with its anatomically superior position in children is especially sensitive to radiation (Duffy and Fitzgerald, 1950, Sikorski and Taylor, 1984).

Concern has been expressed that the lymphoid tissue is particularly susceptible to radiation and growing children tend to exhibit a 'great deal' of lymphoid tissue in Waldeyer's ring in the tonsil and adenoid areas (Watson, 1982).

5.3 DOSIMETRY

In order to reduce radiation dose to patients it is important that both nationally and internationally there are universally agreed units of radiation dose. Units have been selected to be capable of unambiguous definition so that there is agreement as what is to be measured. In this way valid comparisons can be made within the same facility, with measurements in other facilities and with national norms. Important terms in dosimetry include absorbed dose, equivalent dose and effective dose.

Absorbed dose is the energy imparted per unit mass by ionising radiation at a specific point. The S.I. unit of absorbed dose is the Joule per kilogram (J/kg). Absorbed dose is measured in Gray (Gy).

Equivalent Dose is a quantity used for radiation protection purposes that takes into account the different probability of effects that occur with the same absorbed dose by radiations with different radiation weighting factors. Equivalent dose is measured in Sieverts (Sv).

Equivalent dose = Absorbed dose x Radiation weighting factor.

The radiation weighting factors published by the The International Commission On Radiological Protection (ICRP) in 1990, and updated in 2007, for different radiation types are shown in Table 6.

Table 6 Radiation weighting factors

Radiation Type	Radiation Weighting Factor
X-rays, gamma rays and beta particles	1
Fast neutrons (10 keV-100keV) and protons	10
Alpha particles	20

For X-rays, the radiation weighting factor = 1, therefore the equivalent dose measured in Sieverts, is numerically equal to the radiation absorbed dose, measured in Grays.

Effective dose (E) is the sum, over specified tissues, of the products of equivalent dose in a tissue and the tissue weighting factor for that tissue. Effective dose is measure in Sieverts (Sv). Stochastic risk factors are usually stated relative to effective dose.

Effective dose = $\text{Sum}_{\text{specified tissues}}$ (Equivalent dose x Tissue weighting factor)

The ICRP has allocated each tissue a numerical value, known as the tissue weighting factor, based on its radio-sensitivity i.e. the risk of the tissue being damaged by radiation.

The tissue weighting factors recommended by the ICRP in 1990, and updated in 2007, are shown in Table 7.

Table 7 Tissue weighting factors

Tissue	Tissue Weighting Factor (Wt)	Sum of Weighting Factors
Bone-marrow (red), colon, lung, Stomach, Breast, remainder tissues	0.12	0.72
Gonads	0.08	0.08
Bladder, Oesophagus, Liver, Thyroid	0.04	0.16
Bone Surface, Brain, Salivary glands, Skin	0.01	0.04
Total		1.00
Remainder Tissues = Adrenals, extrathoracic (ET) region, gall bladder, heart, kidneys, lymphatic nodes, muscle, oral mucosa, pancreas, prostate, small intestine, spleen, thymus, uterus/cervix)		

5.4 METHODS OF MEASURING RADIATION DOSE

Radiation dose is typically measured using the two recommended dose quantities: Entrance surface dose for individual radiographs, dose-area product for complete examinations. Such measures allow valid and accurate comparisons to be made with previous measurements at the same facility, measurements in other facilities or with nationally agreed norms.

Other dose quantities such as those more closely related to the radiation risk to the patient i.e. effective dose cannot be measured directly rather they are estimated due the various assumptions and uncertainties involved in their estimation which can lead to ambiguity in their expression.

Entrance surface dose is defined as the absorbed dose to air at the point of intersection of the X-ray beam axis with the entrance surface of the patient, including backscattered radiation. The amount of radiation scattered back from a patient into a dosemeter placed on the skin can be substantial. It is essential that this backscattered radiation be completely included in the measurement of entrance surface dose and this is best achieved by using a dosemeter of small volume attached directly to the patient's skin.

Two types of dosemeter are commonly used for measuring entrance surface doses to patients during X-ray examinations namely thermoluminescent dosemeters (TLDs) and ionisation chambers.

TLDs are essentially chips/pellets of lithium fluoride or borate. Absorption of incident X-ray photons causes the ionisation of atoms in the lattice of the crystal. Impurities and crystallographic defects in the material mean there are vacancies within the lattice structure that are capable of accommodating electrons released by ionisation. To determine the amount of radiation that the thermoluminescent detector (TLD) has been exposed to; the chip/pellet from the TLD is placed into a reader containing a dark, heated compartment with a photomultiplier tube attached. Thermal energy produced by the photomultipier tube causes the atoms to vibrate, liberating the trapped electrons, allowing them to return to their ground state. Since this is a transition to a lower energy state, the excess energy is emitted as a photon in the visible region of the spectrum. The photon then produces a current in the photomultiplier tube, which can be measured.

Ionisation chambers provide relatively accurate numerical dose values for absorbed dose, but can only be used to acquire measurements at a few discrete locations due to the size of the chamber i.e. absorbed dose to air, in free air, on the axis of the X-ray beam. Radiation produces ionisation of the air molecules inside the closed chamber, which results in a measurable discharge and hence a direct read-out. Such measurements can then be corrected using appropriate backscatter factors and the inverse square law to estimate entrance surface dose.

TLDs are the dosemeter of choice for direct measurements of entrance surface dose for a number of reasons. A TLD in comparison to an ionisation chamber is physically small and can be attached directly and unobtrusively to the patient's skin with little

interference in patient mobility or comfort. As a result a TLD will fully measure the radiation backscattered from the patient, an essential component of the entrance surface dose. Another reason to use a TLD as compared to an ionisation chamber would be that by leaving a minimal footprint on the radiograph they are unlikely to obscure useful diagnostic information. It is essential that all TLD systems are calibrated to recommended levels to ensure and accuracy and precision.

The specific limitations of ionisation chambers and thermoluminescent detectors illustrated in Table 8 have led to the development of solid state dosemeter systems such as the Patient Skin Dosemeter (Unfors, Billdal, Sweden). Such dosemeters allow for the direct and instantaneous digital measurement of actual patient entrance skin radiation doses. The Patient Skin Dosemeter utilises integrated circuitry with three silicon detector chips 1cm × 0.5cm in size coupled to a small readout device with thin cables. The digital readout unit is about 8cm × 10cm × 2cm. The solid-state detector elements can be placed on the skin surface of patients undergoing radiological examination at an anatomical location, which will be exposed to radiation. The reading is displayed instantaneously. The small sensors leave a minimal footprint on the X-ray image. Complete details of the design are proprietary. Some advantages and disadvantages of a solid state dosemeter are listed in Table 9.

Table 8 Disadvantages of ionisation chamber and thermoluminescent detectors that has led to development of solid state dosemeters

Ionisation Chamber	Thermoluminescent Detector
Sensitivity to static electricity	No instantaneous results
Size limitations	Measurements are time consuming.

Table 9 Advantages and disadvantages of using a solid state dosemeter

Advantages	Disadvantages
Reusable	Relatively new technology
Read-out measurements are instantly produced	Dose gradients are not detectable
Suitable for a wide variety of dose measurements	

5.5 ESTIMATION OF EFFECTIVE DOSE USING PCXMC 2.0

A computer program named PCXMC 2.0 (by use of a Monte Carlo simulation) can be used to estimate organ doses and effective doses in radiographic examinations using current ICRP (International Commission On Radiological Protection) tissue weighting factors (2007). Monte Carlo simulation is based on a class of computational algorithms that rely on repeated random sampling to compute their results (Servomaa and Tapiovaara, 1998). The anatomical data used for simulation in the program are from mathematical hermaphrodite phantom models by Cristy and Eckerman (1987) and describe patients of six different ages: newborn, 1, 5, 10, 15 years old and adult patients.

The PCXMC 2.0 program interface allows free adjustment of the X-ray beam projection and of the X-ray spectrum. X-ray spectrum is specified in terms of peak voltage (kVp), angle of the X-ray tube target and filtration.

To estimate organ or effective dose the program ideally requires a measure of entrance air kerma. The radiation dose quantity can be input as the entrance air kerma specified at the central axis of the X-ray beam entering the phantom, or can

be input as the entrance exposure or dose area product from which the entrance air kerma is estimated. If radiation measurements are not available the program is able to estimate the incident air kerma from the X-ray tube current-time product (Servomaa and Tapiovaara, 1998).

5.6 RADIATION DOSE AND HEALTH RISK

Effective dose and health risk vary according to the type of X-ray apparatus used to acquire a cephalogram, so it is hard to give firm figures, but a recent estimation of radiation dose and health risk when taking an isolated exposure is given in Table 10.

Table 10 Dose of radiation imparted and risk of cancer induction when taking a lateral cephalogram (Moony et al., 2001)

Radiographic Technique	Effective Dose (μSv)	Risk of cancer (per million)
Lateral Cephalogram	3	0.06-0.1

One of the key methods for evaluating the biological effects of radiation is through the use of a dose response curve (Taylor et al., 1988). In the 1980 BEIR III report, the committee on the biological effect of ionising radiation (National Research Council) chose the linear quadratic dose effect graphical model for assessing the health risk of both high and low doses of radiation (Radiation and Council, 2006). The model assumes that there is no minimal threshold in terms of cancer induction and that in time cumulative doses may cause malignant transformation (Taylor et al., 1988).

On the basis of this model the following statement has been made; “Although the radiographic exposure and potential risk is minimal, any reduction in radiographic exposure to the patient from cephalometric radiography would be of obvious benefit” (Forsyth et al., 1996).

5.7 RADIATION PROTECTION

In dental radiography, protection of patients and staff is achieved by three main means. These include justification for any X-ray imaging, dose limitation during irradiation and quality assurance to try and ensure that the image taken is as diagnostic as possible minimising the requirement for a repeat irradiation. As an absolute minimum all radiographs must be justified under current legislation in the UK. It is a legal requirement that no radiological examination should be used unless there is likely to be a benefit in terms of improved prognosis or management of the patient. There are guidelines designed to assist in the justification process so as to avoid unnecessarily irradiating patients.

Indications and selection criteria for cephalometric radiographs are clearly identified by the British Orthodontic Society (Isaacson et al., 2008). Another useful publication is the Faculty of General Dental Practice (UK) 2004 booklet, Selection Criteria in Dental Radiography.

Considering dose limitation the aim would be to ensure all exposures are kept as low as reasonably practicable (ALARP).

With regards to quality assurance a quality standard has been set out by the Faculty Of General Dental Practice (UK). The standard is that no more than 10% of all radiographs taken should be non-diagnostic. Regular audit is recommended to ensure that this standard is met.

5.8 PHANTOM ASSISTED DOSE LIMITATION STUDIES

Different methods of reducing radiation dose in cephalometry have most often been evaluated using head phantoms rather than human subjects. The use of a phantom constructed of “tissue substitute materials” makes it possible to expose the same object several times implementing the planned measures, which allows for direct comparison of several radiographs. This type of research on a human subject would be unethical due to the risks associated with X-ray irradiation. Other uses of phantoms include: Testing the performance of imaging equipment, measuring radiation dosage during therapy, teaching interventional image guided procedures, and servicing equipment in the field (Albertini et al., 2011).

The International Commission on Radiation Units and Measurements (ICRU) defines a ‘tissue substitute’ as “any material that simulates a body of tissue in its interaction with ionising radiation” and a ‘phantom’ as “any structure that contains one or more tissue substitutes and is used to simulate radiation interactions in the human body”.

Phantoms have been used since the beginning of the 20th century but it wasn’t until the 1960s that more reliable tissue substitutes and sophisticated phantoms began to appear such as the Alderson-Rando phantom (Alderson et al., 1962). This is a natural skeleton devoid of extremities with the head containing teeth, the whole skeleton being embedded in a tough thermoplastic material based on synthetic iso-cyanate rubber, which simulates human soft tissue in regard to attenuation of diagnostic and therapeutic X-rays.

One of the most recent head phantoms that has been commissioned for maxillofacial and dental applications is the ATOM max Dental and Diagnostic Head Phantom (Model 711-HN) shown in Figure 7.

Figure 7 ATOM max Dental and Diagnostic Head Phantom with a corresponding CT image

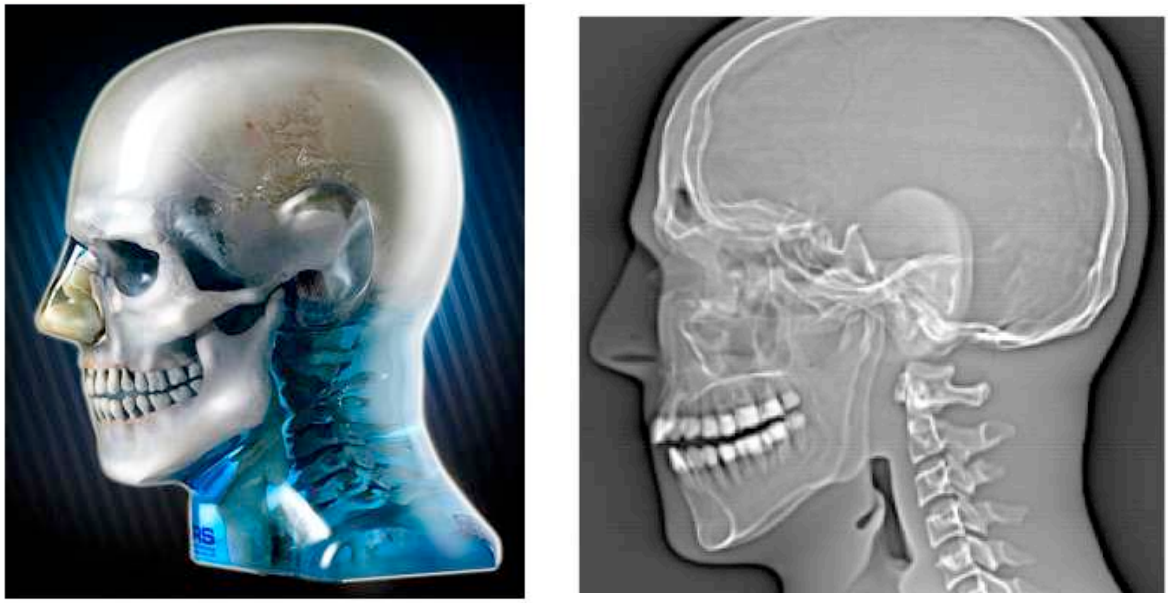

"It is constructed of tissue simulating resins claimed to mimic the X-ray attenuation properties of human tissue for both CT and therapy energy ranges (50kV-25MV). The head phantom approximates the average male human head in both size and structure. It includes anatomy such as the brain, bone, larynx, trachea, sinus, nasal cavities and teeth. The bones contain both cortical and trabecular separation. The teeth include distinct dentine, enamel and root structure including the pulp cavity" (Albertini et al., 2011). The head phantom is mounted on a stand, which allows accurate positioning. This facilitates adjustment in the X-Y-Z axes as well as allowing

rotations about each of these axes. Such a feature is particularly useful for positioning in a cephalostat.

6. CEPHALOMETRIC IMAGE QUALITY

Cephalometric image quality is a major factor influencing the accuracy of cephalometric analysis (Barr and Stephens 1980, Goaz and White 1987). When carrying out any investigation to optimise radiation dose to the patient it is critical that image quality is kept to a standard that will maintain the information of interest to the visual system. Cephalometric image quality is considered in light of visual and geometric characteristics.

6.1 VISUAL CHARACTERISTICS

Visual characteristics such as contrast and density are related to the ability of an image to render optimum detail of different anatomical structures and to allow differentiation between them by means of relative transparency.

Radiographic density of a radiographic image is the degree of blackness rendered. Radiographic density is calculated from the common logarithm of the ratio of the intensity of the light beam of the illuminator striking the image (I_0) to the intensity of the light transmitted through the image (I_t)

$$\text{Density} = \log I_0 / I_t \text{ Viteporn (1995)}$$

Two main factors control the radiographic density of a radiographic image; exposure technique and the processing procedure. The exposure factors related to image density are, tube voltage (kilo-voltage peak, kVp), tube current (milli-amperage, mA),

exposure time (S), focus-film distance (D). The relationship of radiographic image density and these factors is expressed as an equation:

$$\text{Density} = (kVp \times mA \times S) / D$$

Radiographic contrast is the difference in densities between adjacent areas on the radiographic image. Factors controlling radiographic contrast are tube voltage, secondary radiation or scatter radiation and subject contrast.

The kilo-voltage peak (kVp) has the most effect on radiographic contrast. When the kilo-voltage peak is low, the contrast of the image is high, and the image has short-scale contrast. If the kilo-voltage peak is high, the contrast of the image is low and the image has long scale contrast.

The secondary or scatter radiation caused by low energy X-ray beams decreases the contrast by producing fogging of the image. The amount of secondary radiation is directly proportional to the cross-sectional area, thickness and density of the exposed tissues as well as the kilo-voltage peak. Several devices have been incorporated into cephalometric systems to remove secondary radiation, including the use of aluminium filters, lead diaphragms, and grids.

Some manufacturers provide pre-programmed exposure factors consisting of milli-amperage (mA), kilo-voltage peak (kVp) and exposure time (S) which enable image density and contrast to be controlled when object density and thickness are varied.

Variations in the exposure factors depend on the type of X-ray machine, target-image receptor distance, the image receptor type and the grid chosen. Usually the milli-amperage does not exceed 10 mA, the kilo-voltage is about 60-90 kV and the exposure time is not longer than 3 seconds (this differs for digital radiography systems).

6.2 GEOMETRIC CHARACTERISTICS

An X-ray beam is divergent and hence radiates in all directions. Consequently, when it penetrates a three-dimensional object such as a skull, there is always some image unsharpness, image magnification and shape distortion of the object being imaged. These three unwanted effects are known as the geometric characteristics of a radiographic image.

Image unsharpness is classified into three types according to aetiology, namely geometric, motion and material.

Geometric unsharpness is the fuzzy outline in a radiographic image caused by the penumbra. The penumbra appears on images because the focal spot, from which the X-ray beam originates, although small, has a finite area and every point on this area acts as an individual focal spot for the origination of X-ray photons. Therefore, most of the X-ray photons emitted from the focal spot are actually producing a shadow of the object. Factors that influence geometric unsharpness are size of the focal spot,

focus-film distance, and object-film distance. Geometric unsharpness is defined by the following equation:

Geometric unsharpness = (focus spot size x object-film distance)/focus-film distance

In order to decrease the size of the penumbra, the focal spot size and the object-film distance should be decreased whilst increasing the focus-film distance.

Movement of the patient's head and or movement of the tube and film cause motion unsharpness.

Intensifying screens can result in material unsharpness related to the size of the phosphorescent crystals, the thickness of the fluorescent layer, and the film-screen contact. If the intensifying screens are not in tight contact with the film, fluorescent light emerges from the screen in all directions, thus adding to the image distortion.

7. RADIATION DOSE REDUCTION IN LATERAL CEPHALOMETRY

There are a number of known ways to reduce irradiation to the patient during image acquisition in lateral cephalometry. Some of these methods have been outlined in this section.

7.1 SELECTIVE SHIELDING

The aim of selective shielding is that the irradiated field size should be limited to only the areas that yield diagnostic information. Many authors have discussed the proper shielding of patients and collimation to achieve this end. Radiation and absorbed dose measurements for various anatomic sites of the thyroid gland have been reduced by a factor of 1.7 to 37 by combinations of selective shielding and collimation (Eliasson et al., 1984). Thought to be controversial due to hypothesised effect of backscatter within the confines of the collar, the use of a lead collar has been reported to reduce thyroid exposure by 85% without loss of diagnostic information (Block et al., 1977).

7.2 COLLIMATION

Collimation reduces irradiation of the patient by acting to regulate the size and shape of the X-ray beam to those areas of diagnostic interest. Different devices for collimation of cephalometric radiographs have been described that appear to give a sizeable reduction in patient dose (Alpern, 1984). The irradiated area of a patient may be reduced by 55-77% using a properly collimated beam for lateral cephalometric radiographs (Hirschmann, 1985, L'Abee and Tan, 1982).

7.3 QUALITY ASSURANCE

A quality assurance programme ensures that an operator is optimising the use of their equipment and technique with a view to improving the quality and consistency of radiographs. In this way a quality assurance programme aims to ensure that a patient is at minimum risk of being irradiated for a second time due to a poor quality radiograph. A three tiered quality assurance programme has been described based on type and number of films used (Gratt, 1983).

7.4 FILTERS

All X-ray sets used for diagnostic radiography incorporate filters, usually of aluminum or less commonly materials from the rare-earth group of elements, to remove low-energy 'soft' X-rays from the beam thus reducing patient skin dose (Tanimoto et al., 1989). These X-rays are undesirable because they are absorbed by the patient (increasing the patient dose) without contributing to the formation of the radiographic image. A filter aims to match the energy range of the X-ray with the optimal spectral sensitivity of the image receptor used.

Application of filters to reduce dose in cephalometry has been described with the successful implementation of rare-earth filtration using a portion of Lanex intensifying screen to reduce patient irradiation (Tyndall et al., 1988).

7.5 INTENSIFYING SCREENS

Intensifying screens are used in conjunction with X-ray film. They are used to intensify the effect of X-ray photons during exposure of X-ray film and consequently result in reduction of irradiation to the patient. There are two main types; calcium tungstate screens and rare-earth screens. Rare earth has largely superseded the use of calcium tungstate screens. The rare earth types are composed principally of either gadolinium or lanthanum and were introduced into clinical practice in the mid 1970s. The phosphors in these screens have lower atomic numbers than the tungsten in conventional calcium-tungstate screens and consequently lower K-edge absorption energies.

Energy conversion with an intensifying screen is as much as six times more efficient during film exposure than without and as a consequence, patient doses in cephalometric radiography can be reduced using an appropriate screen. (Gratt et al., 1984, Kimura et al., 1987, Lurie, 1981)

7.6 ALTERING EXPOSURE PARAMETERS

An X-ray photon travels with a certain velocity and carries a certain amount of energy, which is directly proportional to the wavelength.

Hard X-rays have short wave lengths and high penetrating power and are produced by a high kilo-voltage peak (kVp) applied across the cathode and anode within the X-ray apparatus. Conversely soft X-rays have long wavelength and low penetrating

power and are produced by the low kilo-voltage peak applied across the cathode and anode.

The quantity of X-ray photons is determined by the amount of bombarded electrons and is controlled by the tube current measured in milli-amperes (mA) flowing through the cathode filament and by the duration of X-ray production or exposure time (measured in seconds).

Altering exposure parameters to reduce radiation dose to the patient involves changing settings or programs on an X-ray apparatus. This involves altering either in combination or isolation the tube voltage (kVp), tube current (mA) and exposure time (S) to ensure as small a patient irradiation as possible whilst producing an image which renders sufficient detail.

It has been proposed that a peak kilo-voltage value of between 60 and 70 kVp would appear to be reasonable for film based cephalometry. "*This range avoids the high skin doses of the lower kilo-voltages, giving a compromise range of contrast suitable for diagnosis and producing a range of X-ray energies well matched to the optimal sensitivity of the radiographic film*" (Horner and Hirschmann, 1990).

7.7 DIGITAL TECHNIQUE

Digital radiography has enabled absorbed doses to be reduced further still (Naslund et al., 1998). The image receptors used in digital radiography have a much wider

dynamic range than film based cephalometry making it possible to use very low exposures without loss of image contrast. The acquisition of a digital image provides the further option of image post-processing, which may also contribute to dose reduction to the patient.

7.7.1 HIGH DENSITY LINE SCAN SOLID STATE DETECTORS

Memory phosphor plates made of barium fluorohalide doped with europium have a high detective quantum efficiency and are a more effective absorber of X-ray photons than the typical X-ray film-intensifying screen combination. A recent study demonstrated a dose reduction of 50% when using memory phosphor plates compared with regular film-screen systems. (Kaeppler et al., 2007).

The effects of dose reduction obtained with photostimulable phosphor digital radiography on the identification of cephalometric landmarks has been measured. A dose reduction of 75% was found not to affect the localization of anatomical landmarks in lateral cephalograms obtained with the use of memory phosphor plates (Naslund et al., 1998).

7.7.2 INTEGRATED FLAT PANEL SYSTEMS

The more recent integrated flat panel systems appear to allow dose reduction however there is a lack of literature studying what contribution this type of technology may impart in reducing patient irradiation in cephalometry. One study has indicated that a direct-digital cephalometric radiography may reduce the

patient's radiation dose by 50% compared with the conventional screen-film technique (Visser et al., 2001)

7.8 IMAGE ENHANCEMENT

The advent of digital radiography has opened the possibility of being able to process digital image data post image acquisition, this has come to be known as post-processing. Any operation that acts to improve, restore, analyse or in some way change a digital image is a form of image post-processing. The different types of post-processing possible are listed in Table 11. It should be noted that post-processing is not possible when using X-ray film as an image receptor unless the image is scanned and saved in a digital format.

The aim of post-processing a radiographic image is to render the information of interest more accessible to the human visual system. With regards to cephalometry this would be the defined cephalometric landmarks of interest. Although a different application, several studies have shown that digital contrast enhancement and filtering may increase diagnostic accuracy for the detection of carious lesions and estimation of lesion depth (Wenzel, 1993, 1998).

A digital image on a screen is a collection of brighter and darker areas, which is composed of a set of cells that are ordered in rows and columns. Individual cells are called picture elements, which have been shortened to ”pixels”. Each of these pixels has a number or digit assigned to it, based upon the amount of exposure the sensor

receives for the corresponding area. The numbers are used by the computer program to assign a different gray scale value to the area, which results in what is seen as an image. Post-processing is essentially where by means of computer software manipulation mathematical formulas are applied to these numerical representations of the digital image to alter their values in a specific way, which results in a new set of pixel values. The resulting set of numbers is used to display the processed or altered image on the monitor screen (Li, 2004).

Table 11 Types of post-processing

Type of post processing	Subcategory
Image restoration	
Image enhancement	a. Brightness and contrast b. Zoom c. Sharpening and smoothing d. Colour e. Digital subtraction radiography
Image analysis	a. Measurement b. Segmentation c. Properties Finding d. Object classification
Image synthesis	
Image compression	

In the majority of current orthodontic imaging software packages, (a specific example being Dolphin Imaging 11) the user has the opportunity to image enhance and edit patient's photographs and radiographs before mounting it to a patient's profile. Typically when mounting a lateral cephalogram an operator is given the opportunity to alter the brightness/contrast, zoom, sharpening/smoothing and colour of the cephalometric image. Brightness and contrast settings can be used to

correct overexposure or underexposure of an image (Van der Stelt, 2005). Exposure conditions can be improved: an overexposed image can be made lighter and conversely the density of an underexposed image can be made darker.

A zoom function allows enlargement or reduction of an image. By using this function the user can potentially make certain details more recognizable. In order to do this the computer duplicates or interpolates rows and columns of the digital image, thus increasing the size of the image on the screen (Van der Stelt, 2005).

The purpose of sharpening and smoothing filters is to improve image quality by removing noise. Noise is irrelevant components of an image that hamper recognition and interpretation of the data of interest (Shrout et al., 1996) and is often categorised as low-frequency (gradual intensity changes) or high frequency noise. Filters that sharpen an image remove low-frequency noise and are intended to enhance the detail in an image. Filters that smooth an image and remove high-frequency noise are intended to reduce the amplitude of small detail in an image.

Colour application of radiographs is a controversial issue in dental digital radiography. Look up tables (LUTs) are assigned to the data that makes up a digital image. Usually a grey scale LUT is used, but colour LUTs can be used. The result gives false-colour images, in that the colours of the image are not those of the object. Humans can distinguish many more colours than shades of grey. Transforming the grey values of a digital image into various colours theoretically enhances the detection of objects within an image (Shi and Li, 2009).

The ability to enhance a radiograph is no excuse to pay less attention to correctly set up an X-ray apparatus prior to image acquisition, but it can help to rescue an image in which exposure conditions were not optimal and thus prevent the need for a retake. This could save the patient from an extra dose of radiation (White and Pharoah, 2004).

AIMS AND OBJECTIVES

AIM

To investigate whether effective dose (and by implication the health risk) can be reduced during the technique of lateral cephalometry without introducing clinically significant error.

OBJECTIVES

The first objective was to determine the minimum effective dose required to obtain a lateral cephalogram capable of being analysed by an on-screen method within a tolerable degree of clinical error.

The second objective was to survey hospital based orthodontic departments in the West Midlands and use the gathered information to estimate what effective dose patients are being exposed to from lateral cephalometric exposures.

MATERIALS AND METHODS

ESTABLISHING TOLERABLE MEASUREMENT ERROR

Opinion of five orthodontic consultants was gathered to define tolerable error (departure) for nine commonly used cephalometric measurements. The questionnaire is attached to the appendix. The responses from the five consultant questionnaires were collated and the median values of the responses for the nine included cephalometric measurements were calculated. The cephalometric measurements and the respective median values are displayed in Table 12.

This information was used for the experimental part of the study for a sample size calculation and to analyse when clinically significant error had affected cephalometric measurements.

Table 12 Median tolerable error for nine cephalometric measurements

Cephalometric Measurement	Median departure* (range)
SNA angle	1^0 (0.5-1^0)
SNB angle	1^0 (0.5-1^0)
ANB angle	0.5^0 (0.25-0.5^0)
SN-Maxillary Plane angle	2^0 (1-3^0)
Maxillary plane-Mandibular Plane angle	3^0 (1-5^0)
Upper Incisors – Maxillary plane angle	3^0 (1-4^0)
Lower incisors-mandibular plane angle	3^0 (1-4^0)
Lower incisors-A-Pogonion length	0.5mm (0.5-1mm)
Nasiolabial angle	5^0 (1-6^0)

*medians calculated from the responses of five consultant orthodontists

IMAGE ACQUISITION

In the first part of the study, lateral cephalograms (images) of a head phantom (Atom Max dental and diagnostic CIRS 711-HN, Virginia) were obtained using a Sirona Orthophos XG 5 DS/Ceph X-ray unit. The head phantom was positioned according to manufacturer guidelines (Figure 8).

Images (twenty-four in total) were obtained for different exposure parameters and added filtration (Table 13); each image was saved as a digital lossless file (Windows Bitmap).

Corresponding to each image entrance surface dose (ESD) was measured at the pre-auricular site on the head phantom using a solid state dosemeter (UNFOR's Patient Skin Dosemeter). To check accuracy and calibrate the readings from the dosemeter seven of the images were each retaken with TLDs used to measure ESD rather than the solid state dosemeter. Due to the known lack of sensitivity of the TLDs they were re-exposed ten times and an average ESD calculated.

Figure 8 Head phantom correctly positioned in the cephalostat

Using the measured ESD, effective dose was estimated for all twenty-four images shown in Table 13 using PCXMC 2.0. To derive these doses a series of four steps was followed on the program interface. The first step was to set the phantom data, geometry data for the X-ray beam, Monte Carlo simulation parameters and field size (Figure 9). The second step was the Monte Carlo simulation (Figure 10), which simulates the path of X-ray photons within the parameters set on the first step. Following the simulation the third step was to specify the X-ray spectrum which was where any filtration added to the X-ray beam was specified as well as the tube potential (Figure 11). The fourth and final step to attain an estimated effective dose was to enter the incident air kerma or entrance surface radiation dose (Figure 12).

Table 13 Exposure parameters and filtration used for each of the head phantom images

Image	Kilovoltage (kVp)	Current (mA)	Exposure time (seconds)	Aluminium Filtration (mmAl)	Entrance Surface Dose (μGy)
1	60	9	9.3	0	19.3
2	60	10	9.3	0	21.0
3	60	12	9.3	0	25.3
4	60	14	9.3	0	29.3
5*	60	16	9.3	0	33.3
6	62	16	9.3	0	39.6
7	64	16	9.3	0	42.1
8	66	16	9.3	0	44.3
9*	69	15	9.3	0	45.8
10	71	15	9.3	0	49.4
11	73	15	9.3	0	52.1
12*	77	14	9.3	0	54.2
13	80	14	9.3	0	56.7
14	84	13	9.3	0	57.1
15*	90	12	9.3	0	64.6
16	60	9	9.3	1	13.3
17	60	9	9.3	2	9.7
18	60	9	9.3	3.2	7.5
19	60	9	9.3	7.19	5.6
20	60	9	9.3	3.72	6.3
21*	69	15	9.3	1	37.5
22*	69	15	9.3	2	29.2
23*	69	15	9.3	4.26	16.7
24	69	15	9.3	7.19	9.6

* Images repeated with thermoluminescent dosimetry

Figure 9 Setup of X-ray simulation

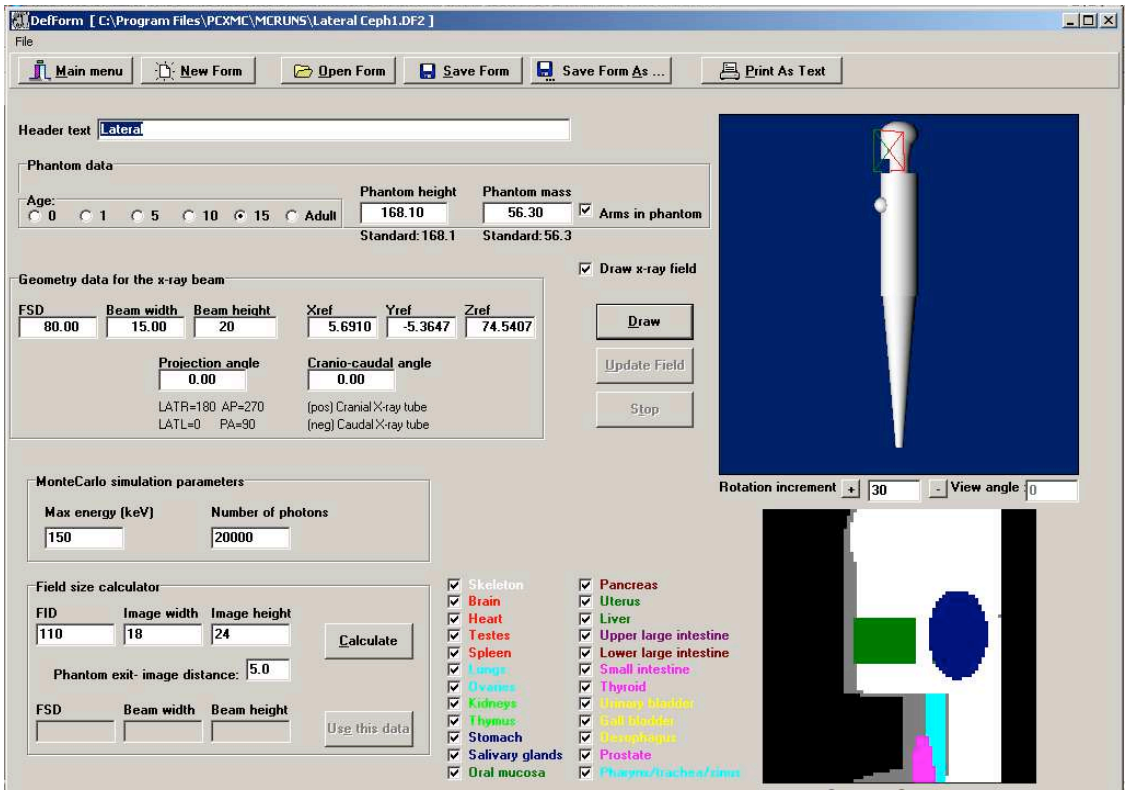

Figure 10 Monte Carlo simulation

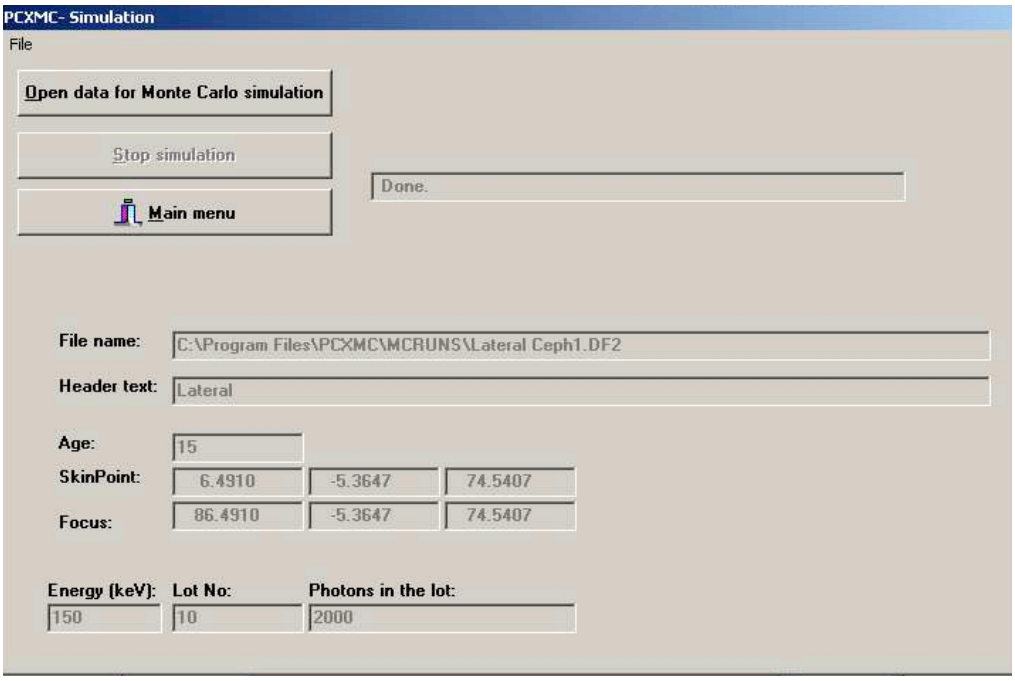

Figure 11 Calculation of X-ray spectrum

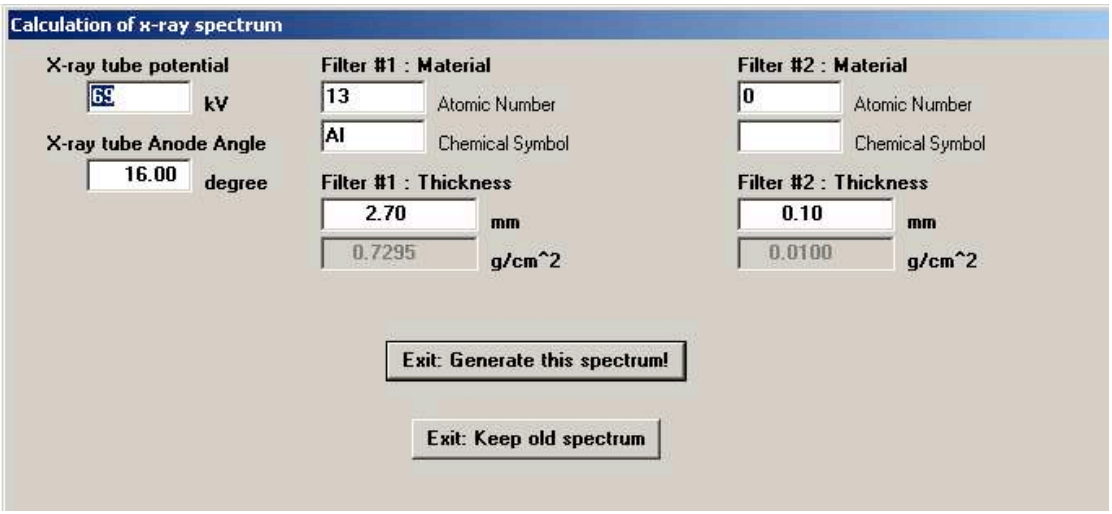

Figure 12 Patient input dose

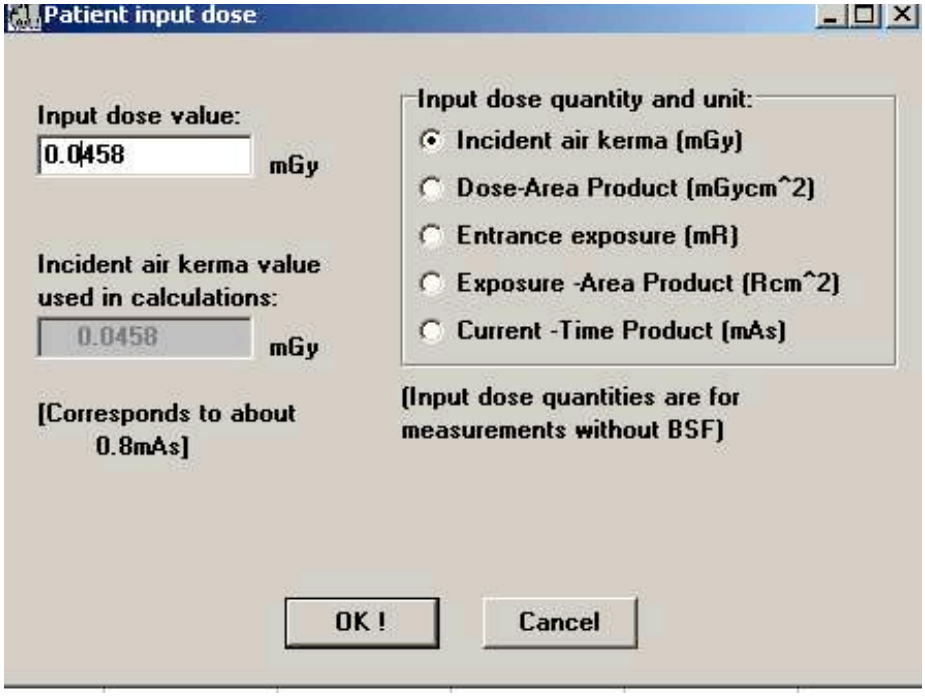

IMAGE SELECTION

From those images acquired a number were selected for image analysis. The first image represented the estimated effective dose most commonly delivered at the orthodontic unit where the research was undertaken (reference dose). The subsequent images selected represented as wide and varied a range of effective dose below the reference dose as possible. A further two repeat images were included in the image set to assess intra-operator reliability.

IMAGE ANALYSIS

Using nQuery Advisor Version 7 (statistics package) it was calculated that recruiting six clinicians to carry out cephalometric analysis will have an 80% power to detect a tolerable difference of 0.5 degrees of the cephalometric measurement ANB assuming a standard deviation of 0.3 degrees with a 5% 2-sided significance level.

The standard deviation of 0.3 degrees of the cephalometric measurement ANB was calculated from six random clinician's cephalometric analyses of an image of the head phantom (Atom Max dental and diagnostic CIRS 711-HN, Virginia). This image was taken at the reference dose.

In light of the sample size calculation, rather than recruiting just six clinicians, ten clinicians were recruited to allow for the possibility of drop out from the study.

The orthodontic clinicians included were three second year specialist trainees, three third year specialist trainees, two senior registrars and two consultants. 1st year specialist registrars were not included in the recruitment group due to insufficient experience in the practice of cephalometric analysis.

For nine consecutive weeks at allocated time points a week apart each operator carried out image analysis of an image on Dolphin Imaging 11 using the same TFT-LCD monitor (Samsung SyncMaster E1720). This was done until all nine images had been analysed. Each image was analysed a week apart to reduce clinician's memory of landmark location and visibility.

Clinicians were blinded to the corresponding effective dose of each image by ensuring that any labels corresponding to radiation dose or exposure parameters were removed from the uploaded images.

Image analysis consisted of carrying out a customised cephalometric analysis to record the angular and linear measurements shown in Table 14.

Whilst carrying out the analysis the operators were also asked to grade each plotted cephalometric landmark as shown in Table 15 using a three point Likert Scale. The Likert Scale has been defined in Table 16. The visibility grading of each cephalometric landmark was carried out to give insight as to whether operators were able to plot cephalometric landmarks within a tolerable amount of error despite increased/reduced visibility.

During image analysis image enhancement tools present in the Dolphin Imaging 11 software were used by the clinicians to help visualisation and localisation of cephalometric landmarks. Image enhancement included adjusting the following image enhancement features of the Lead tools plug-in within the Dolphin Imaging 11 software package: Brightness, Contrast, Gamma, Hue, Saturation, Blur/Sharpen, Emboss. These functions are illustrated on the program interface in Figure 13.

Instruction was provided to the recruited clinicians verbally and by means of an instruction sheet, which has been attached to the appendix.

Table 14 Angular and Linear measurements recorded using the custom cephalometric analysis

Angular Measurement	Linear Measurement
SNA	Lower incisors - APo
SNB	
ANB	
SN-Maxillary Plane	
Upper Incisors-Maxillary Plane	
Lower incisors-Mandibular Plane	
Maxillary-Mandibular Plane	
Nasiolabial	

Table 15 Cephalometric landmarks plotted and graded for visibility

Cephalometric Landmarks	
Sella	A-point
Nasion	ANS
Subnasale	PNS
Upper Lip	Lower incisor tip
B point	Lower incisor root apex
Pogonion	Upper incisor tip
Menton	Upper incisor root apex
Gonion	

Table 16 Likert Scale to grade visibility of cephalometric landmarks

Grade	Description of Grade
1	Impossible to locate cephalometric landmark
2	Difficult to locate cephalometric landmark
3	Definitely possible to locate cephalometric landmark

Figure 13 Image enhancement interface in Dolphin Imaging 11

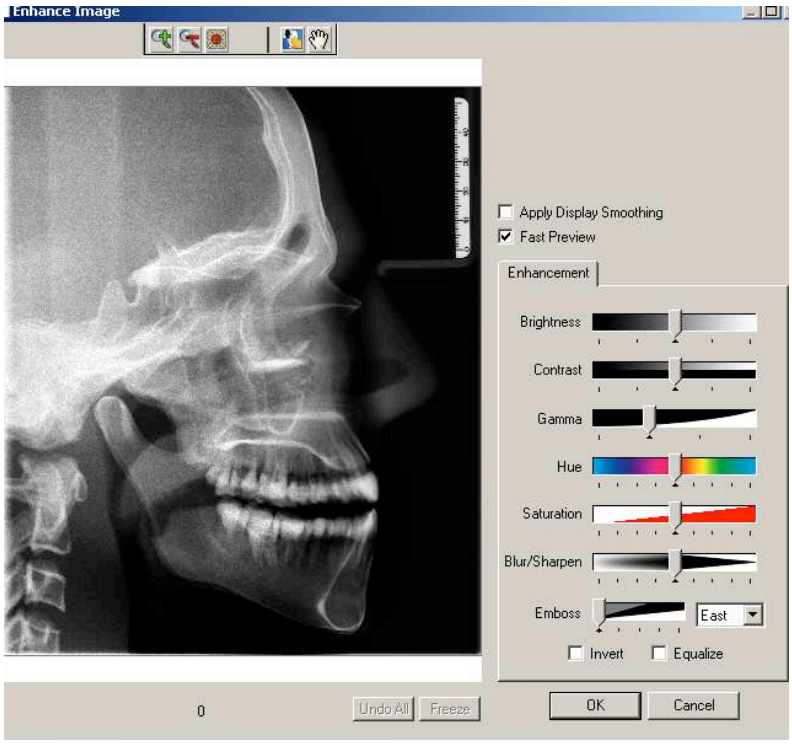

STATISTICAL ANALYSIS

Statistical analysis of the results was carried out using IBM's SPSS Version 20 (statistics package).

A mean was calculated for each of the ten clinician's angular and linear cephalometric measurements at the various effective doses and ninety five percent confidence intervals for the mean defined. A mode was calculated for the visibility grading scores of each of the cephalometric landmarks at the various effective doses. The Wilcoxon Signed Rank Test was used to compare the cephalometric measurements of the images to assess intra-operator reliability.

In order to determine whether an image taken at a specific effective dose was diagnostically acceptable, the mean of each of the cephalometric measurements taken from it had to fall within a defined range. This range was the 95% confidence interval (for the mean) of the equivalent measurement from the image taken at the reference dose, plus or minus the departure defined by the consultant survey.

An 'acceptable' image taken corresponding to the lowest effective dose delivered could thus be determined.

HOSPITAL SURVEY

A survey was carried out at ten hospitals across the West Midlands to facilitate estimation of effective dose imparted from routine lateral cephalometric exposures.

The following information was collected from each of the ten hospitals: The make and model of the X-ray equipment used to take their lateral cephalograms, the type of image receptor the X-ray equipment employs (i.e. plain film, phosphor plate or integrated digital), the exposure parameters typically used during a routine cephalometric exposure (tube potential, current and exposure time).

From the information assimilated PCXMC 2.0 was used to estimate effective dose typically delivered by each hospital unit from a routine lateral cephalometric exposure.

RESULTS

IMAGE ACQUISITION

A total of twenty-four cephalometric images were taken for various combinations of tube potential, tube current, exposure time and aluminium filtration. From the measurements of ESD an effective dose was calculated using PCXMC 2.0. These data are shown in Table 17.

IMAGE SELECTION

From the acquired images an image set was constructed for image analysis, which is shown in Table 18. The first image included represented the reference dose i.e. 0.6μSv. The subsequent six images were included to correspond to a range of effective dose below the reference dose. Each of the cephalograms chosen for image analysis are shown in Figures 14 to 20 respectively. Two further repeat images were included corresponding to the effective dose of 0.60μSv and 0.29μSv respectively to study the intra-operator reliability.

Table 17 Acquired cephalograms with specified filtration, exposure parameters used and calculated corresponding estimated effective dose

Image	Kilovoltage (kVp)	Current (mA)	Exposure time (seconds)	Aluminium Filtration (mmAl)	Entrance Surface Dose (μGy)	Effective Dose (μSv)
1	60	9	9.3	0	19.3	0.22
2	60	10	9.3	0	21.0	0.24
3	60	12	9.3	0	25.3	0.29
4	60	14	9.3	0	29.3	0.33
5	60	16	9.3	0	33.3	0.38
6	62	16	9.3	0	39.6	0.52
7	64	16	9.3	0	42.1	0.55
8	66	16	9.3	0	44.3	0.58
9	69	15	9.3	0	45.8	0.60*
10	71	15	9.3	0	49.4	0.65
11	73	15	9.3	0	52.1	0.69
12	77	14	9.3	0	54.2	0.80
13	80	14	9.3	0	56.7	0.75
14	84	13	9.3	0	57.1	0.75
15	90	12	9.3	0	64.6	1.10
16	60	9	9.3	1	13.3	0.15
17	60	9	9.3	2	9.7	0.11
18	60	9	9.3	3.2	7.5	0.09
19	60	9	9.3	7.19	5.6	0.06
20	60	9	9.3	3.72	6.3	0.07
21	69	15	9.3	1	37.5	0.49
22	69	15	9.3	2	29.2	0.38
23	69	15	9.3	4.26	16.7	0.22
24	69	15	9.3	7.19	9.6	0.13

* Reference dose

Table 18 Image set for image analysis

Image	Kilovoltage (kV)	Current (mA)	Exposure Time (seconds)	Aluminium Filtration (mmAl)	Effective Dose (μSv)
9	69	15	9.3	0	0.60*
21	69	15	9.3	1	0.49
22	69	15	9.3	2	0.38
3	60	12	9.3	0	0.29
23	69	15	9.3	4.26	0.22
24	69	15	9.3	7.19	0.13
19	60	9	9.3	7.19	0.06
9**	69	15	9.3	0	0.60*
3**	60	12	9.3	0	0.29

* Reference dose
** Repeat images included for study of intra-operator reliability

Figure 14 Cephalogram corresponding to a 0.60μSv effective dose

Figure 15 Cephalogram corresponding to a 0.49μSv effective dose

Figure 16 Cephalogram corresponding to a 0.38μSv effective dose

Figure 17 Cephalogram corresponding to a 0.29μSv effective dose

Figure 18 Cephalogram corresponding to a 0.22μSv effective dose

Figure 19 Cephalogram corresponding to a 0.13μSv effective dose

Figure 20 Cephalogram corresponding to a 0.06μSv effective dose

IMAGE ANALYSIS

For each of the nine images analysed, the mean, standard deviation and 95% confidence interval for the mean for each cephalometric measurement at each effective dose were calculated.

The cephalometric measurements for angle SNA (Table 19), angle SNB (Table 20), angle ANB (Table 21), SN-Maxillary Plane angle (Table 22), Maxillary-Mandibular Plane angle (Table 23), Upper Incisors to Maxillary Plane angle (Table 24), Lower Incisors to Mandibular Plane angle (Table 25), Lower Incisors to A-Pogonion (Table 26) and Nasiolabial angle (Table 27) all were not affected by clinically significant error at any of the effective doses ranging from 0.6µSv-0.06µSv.

These findings are made on the basis that the mean of the cephalometric measurements taken at each of the effective doses ranging from 0.6µSv-0.06µSv all fall within the predefined ranges i.e. the 95% confidence interval (for the mean) of the equivalent measurement from the image taken at the reference dose, plus or minus the departure defined by the consultant survey.

Table 19 Results for angle SNA

Effective Dose (μSv)	Mean (degrees)	Standard Deviation (degrees)	95% Confidence interval for the mean (degrees)
0.6	96.5	0.5	96.1 to 96.8
0.49	96.6	0.9	96.0 to 97.3
0.38	96.3	0.6	95.9 to 96.7
0.29	96.7	0.7	96.2 to 97.2
0.22	96.1	0.7	95.6 to 96.7
0.13	96.4	0.7	95.9 to 96.9
0.06	97.0	0.7	96.5 to 97.5

Acceptable range 95.1^0 to 97.8^0

Table 20 Results for angle SNB

Effective Dose (μSv)	Mean (degrees)	Standard Deviation (degrees)	95% Confidence interval for the mean (degrees)
0.60	92.7	0.8	92.1 to 93.2
0.49	92.7	0.9	92.0 to 93.3
0.38	92.7	1.0	92.0 to 93.4
0.29	92.8	0.5	92.4 to 93.2
0.22	92.4	0.5	92.0 to 92.7
0.13	92.6	0.9	91.9 to 93.2
0.06	93.0	0.6	92.6 to 93.5

Acceptable range 91.1^0 to 94.2^0

Table 21 Results for angle ANB

Effective Dose (μSv)	Mean (degrees)	Standard Deviation (degrees)	95% Confidence interval for the mean (degrees)
0.60	3.8	0.8	3.3 to 4.4
0.49	3.9	1.2	3.1 to 4.8
0.38	3.6	1.0	2.9 to 4.2
0.29	3.9	0.7	3.4 to 4.4
0.22	3.8	0.7	3.3 to 4.3
0.13	3.9	0.4	3.6 to 4.2
0.06	4.0	0.6	3.5 to 4.4

Acceptable range 2.7^0 to 4.9^0

Table 22 Results for SN-Maxillary Plane angle

Effective Dose (μSv)	Mean (degrees)	Standard Deviation (degrees)	95% Confidence interval for the mean (degrees)
0.60	-4.7	4.4	-7.1 to 1.5
0.49	-5.0	5.7	-9.1 to -1.0
0.38	-4.8	4.0	-7.7 to -2.0
0.29	-4.4	4.6	-6.4 to 0.1
0.22	-5.5	4.6	-8.8 to -2.2
0.13	-6.2	4.6	-9.5 to -3.0
0.06	-5.8	4.4	-8.9 to -2.6

Acceptable range -3.9^0 to -9.9^0

Table 23 Results for Maxillary-Mandibular Plane angle

Effective Dose (μSv)	Mean (degrees)	Standard Deviation (degrees)	95% Confidence interval for the mean (degrees)
0.60	28.9	4.1	25.9 to 31.8
0.49	29.0	5.3	25.2 to 32.7
0.38	29.3	3.9	26.5 to 32.1
0.29	28.5	4.2	25.5 to 31.5
0.22	30.0	4.5	26.8 to 33.2
0.13	21.4	4.5	28.2 to 34.5
0.06	30.2	4.4	27.1 to 33.3

Acceptable range 22.9^0 to 34.8^0

.

Table 24 Results for Upper Incisors to Maxillary Plane angle

Effective Dose (μSv)	Mean (degrees)	Standard Deviation (degrees)	95% Confidence interval for the mean (degrees)
0.60	109.3	4.0	106.5 to 112.1
0.49	108.9	6.0	104.6 to 113.2
0.38	109.9	3.4	107.5 to 112.3
0.29	110.3	4.5	107.1 to 113.5
0.22	108.5	6.0	104.2 to 112.8
0.13	107.7	5.3	103.9 to 111.5
0.06	109.5	4.8	106.0 to 113.0

Acceptable range 103.5^0 to 115.1^0

Table 25 Results for Lower Incisors to Mandibular Plane angle

Effective Dose (μSv)	Mean (degrees)	Standard Deviation (degrees)	95% Confidence interval for the mean (degrees)
0.60	85.0	1.8	83.7 to 86.4
0.49	83.5	1.6	82.4 to 84.7
0.38	83.9	1.0	83.2 to 84.6
0.29	85.7	2.4	84.3 to 87.1
0.22	83.9	2.0	83.1 to 84.6
0.13	83.5	1.1	82.6 to 84.3
0.06	84.0	1.4	83.0 to 85.1

Acceptable range 80.7^0 to 89.4^0

Table 26 Results for measurement Lower Incisors to A-Pogonion

Effective Dose (μSv)	Mean (mm)	Standard Deviation (degrees)	95% Confidence interval for the mean (mm)
0.60	4.5	0.4	4.1 to 4.8
0.49	4.5	0.3	4.3 to 4.7
0.38	5.3	1.9	3.9 to 6.6
0.29	5.3	3.1	3.1 to 7.6
0.22	4.6	0.2	4.4 to 4.8
0.13	4.5	0.5	4.1 to 4.9
0.06	4.3	0.6	3.9 to 4.7

Acceptable range 3.6mm-5.3mm

Table 27 Results for Nasiolabial angle

Effective Dose (μSv)	Mean (degrees)	Standard Deviation (degrees)	95% Confidence interval for the mean (degrees)
0.60	116.6	4.5	113.3 to 119.8
0.49	116.7	7.6	111.3 to 122.1
0.38	115.0	4.6	111.7 to 118.3
0.29	116.2	8.2	110.3 to 122.1
0.22	117.8	8.4	111.7 to 123.8
0.13	117.3	7.9	111.7 to 123.0
0.06	116.9	4.6	113.6 to 120.2

Acceptable range 108.3^0 to 124.8^0

INTRA-OPERATOR RELIABILITY

Wilcoxon signed rank tests indicate that there was no significant intra-operator clinical error on repeating any of the cephalometric measurements at the control effective dose of 0.60μSv (Table 28)

At the effective dose of 0.29μSv no significant clinical error was found on repeating cephalometric measurements angle SNA, angle SNB, angle ANB, Maxillary Plane-Mandibular Plane angle, Lower Incisors-Mandibular Plane angle, Lower Incisors to A-Pogonion length, Nasiolabial angle however significant intra-operator error was found to affect the measurements SN-Maxillary plane angle ($P<0.05$) and also the Upper Incisor to Maxillary Plane angle ($P<0.01$), which is shown in Table 29.

Table 28 Intra-operator reliability at an effective dose of 0.60 μSv

Cephalometric Measurement	Z	P
SNA angle	-0.712	0.476
SNB angle	0	1.00
ANB angle	-0.949	0.342
SN-Maxillary Plane angle	-1.275	0.202
Maxillary plane-Mandibular Plane angle	-1.070	0.285
Upper Incisors – Maxillary plane angle	-0.714	0.475
Lower incisors-mandibular plane angle	-1.784	0.074
Lower incisors-A-Pogonion length	-0.418	0.676
Nasiolabial angle	-1.632	0.103

* P<0.05 **P<0.01

Table 29 Intra-operator reliability at an effective dose of 0.29 μSv

Cephalometric Measurement	Z	P
SNA angle	-1.010	0.313
SNB angle	-0.665	0.506
ANB angle	-0.205	0.838
SN-Maxillary Plane angle	-2.142	0.032*
Maxillary plane-Mandibular Plane angle	-1.785	0.074
Upper Incisors – Maxillary plane angle	-2.599	0.009**
Lower incisors-mandibular plane angle	-1.989	0.047
Lower incisors-A-Pogonion length	-0.070	0.944
Nasiolabial angle	-1.172	0.241

* P<0.05 **P<0.01

CEPHALOMETRIC LANDMARK VISIBILITY GRADING

The mode of the visibility grading for each cephalometric landmark at each effective dose was calculated for all ten recruited clinicians the results are shown in Table 30. The visibility grading for cephalometric landmarks Sella, Nasion, Subnasale, B-point, Pogonion, Menton, Gonion, A-point, ANS, PNS, Lower incisor tip, Lower incisor root apex, Upper incisor tip and Upper incisor root apex at each of the effective doses 0.60μSv, 0.49μSv, 0.38μSv, 0.29μSv, 0.22μSv, 0.13μSv and 0.06μSv was found to range from difficult to locate (Grade 2) to definitely possible to locate (Grade 3). The same findings were not found for the cephalometric landmark upper lip point. The cephalometric landmark upper lip point was found to be impossible to locate (Grade 1) by a majority of clinicians at 0.60μSv, 0.49μSv and 0.06μSv.

Table 30 Mode scores from visibility grading of cephalometric landmarks

Cephalometric Landmark	Effective Dose (μSv)						
	0.60	0.49	0.38	0.29	0.22	0.13	0.06
Sella	3	3	3	3	3	3	3
Nasion	3	3	3	3	3	3	3
Subnasale	3	3	3	3	3	3	3
Upper Lip	1*	1*	2	2	2	2	1*
B-Point	3	3	3	3	3	3	3
Pogonion	3	3	3	3	3	3	3
Menton	3	3	3	3	3	3	3
Gonion	3	3	3	3	3	3	3
A-Point	3	3	3	3	3	3	3
ANS	3	3	3	3	3	3	3
PNS	3	2	3	3	3	3	2
Lower incisor tip	3	3	3	3	3	3	3
Lower incisor root apex	3	2	2	2	2	2	2
Upper incisor tip	3	3	3	3	3	3	3
Upper incisor root apex	3	2	3	2	2	2	3

*Impossible to locate landmark

HOSPITAL SURVEY

Using the information collected from the hospital survey an estimation of effective dose delivered on carrying out a lateral cephalometric exposure at each of the ten orthodontic hospital units was calculated using PCXMC 2.0. The estimated effective doses for each unit surveyed are shown in Table 31. For image capture, two of the units were using cephalostats utilising an integrated flat panel detector whilst the remaining eight were using a memory phosphor plate.

Table 31 Estimated effective dose for a lateral cephalometric exposure at each hospital unit surveyed

Hospital	Image receptor	Effective dose (μSv)
1	Integrated digital detector	2.4
2	Phosphor Plate	1.4
3	Phosphor Plate	1.4
4	Phosphor Plate	1.0
5	Phosphor Plate	0.9
6	Phosphor Plate	0.9
7	Phosphor Plate	0.7
8	Integrated digital detector	0.6*
9	Phosphor Plate	0.6
10	Phosphor Plate	0.5

* Reference dose

DISCUSSION

Contemporary digital lateral cephalometry has been applied to conventional radiography with the benefits of image storage, transmission and processing. It is known that there is a wide dynamic range available at which radiographs can be taken as compared to using plain film as an image receptor (Naslund et al., 1998).

Using a contemporary digital X-ray apparatus a laboratory study was carried out to determine the minimum radiation dose required to obtain a lateral cephalogram capable of being analysed by an on-screen method within an acceptable degree of clinical error.

A set of recruited clinicans carried out a custom cephalomteric analysis and scored specified cephalometric landmarks for their visibility on a series of digital lateral cephalograms taken of a tissue equivalent head phantom at different effective doses. All lateral cephalograms included were taken at and below the effective dose most commonly imparted by the radiographers using the X-ray apparatus in the research centre.

From the statistical analysis of the results, despite difficulty visualising certain cephalometric landmarks, effective dose reduction from 0.60µSv ranging to 0.49µSv, 0.38µSv, 0.29µSv, 0.22 µSv and 0.06µSv respectively did not impart clinically significant error to any of the cephalometric measurements studied; angle SNA, angle SNB, angle ANB, SN-Maxillary Plane angle, Maxillary-Mandibular Plane angle,

Upper Incisors to Maxillary Plane angle, Lower Incisors to Mandibular Plane angle, Lower Incisors to A-Pogonion length and Nasiolabial angle.

The results of the Wilcoxon signed rank test used to study intra-operator reliability at the effective dose of 0.6μSv and 0.29μSv indicates that there is a greater scope for error in consistency of landmark plotting at a reduced effective dose. This would indicate that greater vigilance is required by the operator when plotting landmarks at a reduced effective dose such as those that make up the SN-Maxillary Plane angle ($P<0.05$) and also the Upper Incisor to Maxillary Plane angle ($P<0.01$).

Taking all factors into consideration this cephalometric study would indicate using an X-ray apparatus with an integrated digital detector for image acquisition and using an orthodontic software package to mount, enhance and analyse it, an effective dose of 0.06μSv may well be utilisable with due care and diligence by the operator. Interestingly this is a factor of fifty times lower than the effective dose of 3μSv quoted for a typical lateral cephalometric exposure in a recent British Orthodontic Society guideline document (Isaacson et al., 2008).

The findings of the hospital survey demonstrate that all units surveyed are delivering an effective dose per lateral cephalogram that is lower than the effective dose of 3μSv (cited in the aforementioned British Orthodontic Society guideline document). Though encouraging that the effective doses recorded in the hospital survey are all lower than this, there is a wide range of effective dose being delivered across all ten orthodontic units surveyed. The orthodontic unit delivering the highest effective

dose of 2.4µSv per lateral cephalogram is a factor of 4.8 times higher than the orthodontic unit delivering the lowest effective dose of 0.5µSv per lateral cephalogram. It could be argued that this may be due to the different type of image receptor used in each of these orthodontic units, however there are effective doses recorded between 0.6µSv and 2.4µSv for units using an integrated flat panel detector image receptor type and 0.5 µSv and 1.4 µSv for those orthodontic units using a memory phosphor plate image receptor type.

The findings of the hospital survey would indicate that some of these hospital units have scope to optimise effective dose during routine lateral cephalometric exposures.

From calculations carried out using the suggested model (Radiation and Council, 2006) health risk has been calculated for adolescent males and females representive of the highest effective dose recorded from the hospital survey (2.4µSv), the effective dose most commonly imparted by the research center (0.6µSv) and the lowest effective dose that could be used without imparting clinically significant error to cephalometric analysis from the laboratory study (0.06µSv).

Calculations have been done to show both Lifetime risk of cancer induction (Table 32) and Lifetime risk of cancer induced mortality (Table 33)

Table 32 Lifetime risk of cancer incidence

Patient	Effective Dose (µSv)	Risk Factor for all Fatal Cancer (all cancers)	Lifetime risk of cancer incidence
Male	2.4	0.0001182	1 in 3,500,000
	0.6	0.0001182	1 in 14,000,000
	0.06	0.0001182	1 in 140,000,000
Female	2.4	0.0002064	1 in 2,000,000
	0.6	0.0002064	1 in 8,000,000
	0.06	0.0002064	1 in 80,000,000

Table 33 Lifetime risk of fatal cancer

Patient	Effective Dose (µSv)	Risk Factor for all Fatal Cancer (all cancers)	Lifetime Risk of Fatal Cancer
Male	2.4	0.0000603	1 in 7,000,000
	0.6	0.0000603	1 in 28,000,000
	0.06	0.0000603	1 in 280,000,000
Female	2.4	0.0000914	1 in 4,500,000
	0.6	0.0000914	1 in 18,000,000
	0.06	0.0000914	1 in 180,000,000

Theoretically, if the hospital that typically imparts an estimated effective dose of 2.4µSv per lateral cephalogram were able to reduce the effective dose to 0.06µSv this would relate to the following reduction in risks of lifetime risk of cancer induced mortality for patients shown in Table 34

Table 34 Risk reduction for lifetime risk of cancer induced mortality 2.4µSv => 0.06µSv

Male	Female
40x risk reduction	40x risk reduction

Theoretically if the research center that typically imparts an estimated effective dose of 0.6µSv per lateral cephalogram were able to reduce the effective dose to 0.06µSv this would relate to the following reduction in risks of lifetime risk of cancer induced mortality for patients shown in Table 35:

Table 35 Risk reduction for lifetime risk of cancer induced mortality 0.6µSv => 0.06µSv

Male	Female
10x risk reduction	10x risk reduction

The effective doses and associated health risks may appear small particularly when taking into consideration the natural risk of fatal cancer in humans is approximately one in four (Isaacson et al., 2008) , however It is important to consider that approximately 150,000 lateral cephalograms are taken in the United Kingdom per year (Hart et al., 2008, NHS, 2003) and that the risk of cancer induction is potentially going to vary from one individual to another. The effects of radiation have also been found to be cumulative (Health Risks from Exposure to Low Levels of Ionizing Radiation: BEIR VII Phase 2, 2006). This is particularly noteworthy because some orthodontic patients will have more than one lateral cephalometric exposure during a course of orthodontic treatment along with other diagnostic radiographs, which all adds to the cumulative health risk experienced during a course of orthodontic treatment.

The findings of this study highlight the fact that with digital lateral cephalometry we have a wide dynamic range as compared to lateral cephalometry utilising radiographic film as an image receptor. Whilst giving the potential for dose reduction

it could mean that if not utilised properly patients are being exposed to unnecessarily high radiation doses. It is extremely important that dose optimisation is borne in mind when using digital technology.

The study should act as a reminder that a lateral cephalogram's justification is to demonstrate relevant cephalometric landmarks which will facilitate cephalometric analysis. Though there is a chance of discovering a potentially life-affecting pathology on a lateral cephalogram (Moffitt, 2011), it is arguably not acceptable to expose patients to unnecessarily high radiation doses for the purposes of detecting an incidental finding.

LIMITATIONS OF STUDY

This study is not without recognised limitations. The findings are representive of one tissue equivalent phantom. It is recognised that however well a phantom mimics human anatomy a human subject would always be preferred but may not be practical due to the experimental difficulties of carrying out such an investigation. Using a single phantom may also have meant that the recruited clinicians may have begun to memorise the location of cephalometric landmarks particularly from cephalograms where they were well visualised. To reduce this predicted effect each cephalogram was analysed a week apart. It is also recognised that using a single phantom does not represent individual patient variation (Kimura et al., 1987).

This study focused on introduction of error to angular and linear cephalometric measurements. A weakness of this approach is that if cephalometric points are plotted incorrectly one could still attain an angular or linear measurement, which appears to be within the range of tolerable error. The fact that the cephalometric landmark or landmarks have been plotted incorrectly may therefore be hidden.

FUTURE WORK

This study highlights that effective dose may be reduced to patients during routine lateral cephalometric exposures in the West Midlands, however further research in this area would be of benefit.

This work has the potential to progress to a future patient based trial that would address some of the limitations of this study. Such work may significantly change current thinking and practice not only for clinicians and radiographers taking cephalometric images but also for manufacturers of X-ray apparatus.

CONCLUSIONS

The aim of this study was to investigate whether health risk may be reduced to a patient population when taking a lateral cephalogram.

In conclusion the findings of the experimental part of the study and the hospital survey confirm that a reduction in effective dose and by implication health risk may be possible during lateral cephalometry.

To reduce and optimise effective dose to patients; an appreciation of the wide dynamic range of a typical digital image receptor as compared to a film based image receptor is paramount, clinicians and radiographers should appreciate that a lateral cephalogram need simply demonstrate the cephalometric landmarks required for the purposes of cephalometric analysis, it is not acceptable to overexpose a patient for the purpose of identifying incidental pathology.

REFERENCES

Ahlqvist, J., Eliasson, S. and Welander, U. (1986)
The effect of projection errors on cephalometric length measurements.
Eur J Orthod*,* 8: (3): 141-148.

Albertini, F., Casiraghi, M., Lorentini, S., Rombi, B. and Lomax, A.J. (2011)
Experimental verification of IMPT treatment plans in an anthropomorphic phantom in the presence of delivery uncertainties.
Phys Med Biol*,* 56: (14): 4415-4431.

Alderson, S.W., Lanzl, L.H., Rollins, M. and Spira, J. (1962)
An instrumented phantom system for analog computation of treatment plans.
Am J Roentgenol Radium Ther Nucl Med*,* 87: 185-195.

Alpern, M.C. (1984)
Clinical radiography in the orthodontic practice.
Angle Orthod*,* 54: (3): 233-246.

Athanasiou, A. (1995)
Orthodontic cephalometry.
London: Mosby-Wolfe.

Barr, J.H. and Stephens, R.G. (1980)
Dental Radiology
WB Saunders: Philadelphia

Baumrind, S. and Frantz, R.C. (1971)
The reliability of head film measurements. 1. Landmark identification.
Am J Orthod*,* 60: (2): 111-127.

Block, A.J., Goepp, R.A. and Mason, E.W. (1977)
Thyroid radiation dose during panoramic and cephalometric dental X-ray examinations.
Angle Orthod*,* 47: (1): 17-24.

Broadbent, B.H. (1931)
A new x-ray technique and its application to orthodontia.
Angle Orthod*,* 1: (2): 45-66.

Chen, Y.J., Chen, S.K., Yao, J.C. and Chang, H.F. (2004)
The effects of differences in landmark identification on the cephalometric measurements in traditional versus digitised cephalometry.
Angle Orthod*,* 74: (2): 155-161.

Cohen, A.M. (1984)
Uncertainty in cephalometrics.
Br J Orthod*,* 11: (1): 44-48.

Cristy, M.E., K.F. (1987)
"Specific Absorbed Fractions Of Energy At Various Ages From Internal Photon Sources".
Tennessee, Oak Ridge National Laboratory.

Duffy, B.J., Jr. and Fitzgerald, P.J. (1950)
Cancer of the thyroid in children: a report of 28 cases.
J Clin Endocrinol Metab*,* 10: (10): 1296-1308.

Eliasson, S., Julin, P., Richter, S. and Strenstrom, B. (1984)
Radiation absorbed doses in cephalography.
Swed Dent J*,* 8: (1): 21-27.

Forsyth, D.B., Shaw, W.C. and Richmond, S. (1996)
Digital imaging of cephalometric radiography, Part 1: Advantages and limitations of digital imaging.
Angle Orthod*,* 66: (1): 37-42.

Gibbs, S.J., Pujol, A., Jr., Chen, T.S. and James Jr, A. (1988)
Patient risk from intraoral dental radiography.
Dentomaxillofac Radiol*,* 17: (1): 15-23.

Gill, D. (2008)
Orthodontics at a Glance.
John Wiley & Sons.

Goaz, P.W. and White, S.C. (1987)
Oral Radiology: Principles and Interpretation.
CV Mosby: St Louis.

Gratt, B.M. (1983)
Recommendations for quality assurance in dental radiography.
Oral Surg Oral Med Oral Pathol*,* 55: (4): 421-426.

Gratt, B.M., White, S.C., Packard, F.L. and Petersson, A.R. (1984)
An evaluation of rare-earth imaging systems in panoramic radiography.
Oral Surg Oral Med Oral Pathol*,* 58: (4): 475-482.

Greer, D.F. (1972)
Determination and analysis of absorbed doses resulting from various intraoral radiographic techniques.
Oral Surg Oral Med Oral Pathol*,* 34: (1): 146-162.

Hart, D., Wall, B.F., Hillier, M.C., Shrimpton, P.C. (2008)
"Frequency and Collective Dose for Medical and Dental X-ray Examinations in the UK, 2008".
Health Protection Agency UK.

Health Risks from Exposure to Low Levels of Ionizing Radiation
BEIR VII Phase 2 (2006)
The National Academies Press.

Hirschmann, P. (1985)
Reduction of the dose to patients during lateral cephalometric radiography. Report of a Joint Working Party of the British Society for the Study of Orthodontics and the British Society of Dental and Maxillofacial Radiology.
Br Dent J*,* 158: (11): 415.

Hixon, E. (1960)
Cephalometrics and longitudinal research.
Am J Orthod*,* 46: 36-42.

Hofrath, H. (1931)
Die Bedeutung Der Roentgenfern und Abstandsaufnahme fur die Diagnostik der Kieferanomalien.
Fortschr Orthod, 1: 232-248.

Horner, K. and Hirschmann, P.N. (1990)
Dose reduction in dental radiography.
J Dent, 18: (4): 171-184.

Houston, W.J., Maher, R.E., McElroy, D. and Sherriff, M. (1986)
Sources of error in measurements from cephalometric radiographs.
Eur J Orthod, 8: (3): 149-151.

Isaacson, K.J., Thom, A.R., Horner, K. and Whaites, E. (2008)
"Orthodontic Radiographs - Guidelines".
British Orthodontic Society.

Kaeppler, G., Dietz, K. and Reinert, S. (2007)
Possibilities of dose reduction in lateral cephalometric radiographs and its effects on clinical diagnostics.
Dentomaxillofac Radiol, 36: (1): 39-44.

Kimura, K., Langland, O.E. and Biggerstaff, R.H. (1987)
The evaluation of high-speed screen/film combinations in cephalometric radiography.
Am J Orthod Dentofacial Orthop, 92: (6): 484-491.

L'Abee, E.M. and Tan, H.T. (1982)
Improved radiation hygiene in lateral cephalometry and a method to obtain good reproduction of the soft tissue profile.
J Clin Orthod, 16: (6): 381-386.

Lakhani, N. (2010)
"High radiation puts child X-ray patients at risk".
The Independent.

Li, G. (2004)
Comparative investigation of subjective image quality of digital intraoral radiographs processed with 3 image-processing algorithms.
Oral Surg Oral Med Oral Pathol Oral Radiol Endod*,* 97: (6): 762-767.

Lurie, A.G. (1981)
JCO interviews Dr. Alan G. Lurie on risk/benefit considerations in orthodontic radiology.
J Clin Orthod*,* 15: (7): 469-475, 478-484.

Martin, C.J. and Sutton, D.G. (2002)
Practical Radiation Protection In Health Care.
Oxford University Press.

McClure, S.R., Sadowsky, P.L., Ferreira, A. and Jacobson, A. (2005)
Reliability of Digital Versus Conventional Cephalometric Radiology: A Comparative Evaluation of Landmark Identification Error.
Seminars in orthodontics*,* 11: (2): 98-110.

Midtgard, J., Bjork, G. and Linder-Aronson, S. (1974)
Reproducibility of cephalometric landmarks and errors of measurements of cephalometric cranial distances.
Angle Orthod*,* 44: (1): 56-61.

Moffitt, A.H. (2011)
Discovery of pathologies by orthodontists on lateral cephalograms.
Angle Orthod*,* 81: (1): 58-63.

Moony, J., Hirschmann, P.N., Williams, M., Gill, J.R., Walker, A., Hudson, A.P. and Napier, I.D. (2001)
Dental practitioners on the safe use of X-Ray equipment.
Department Of Health UK

Naslund, E.B., Kruger, M., Petersson, A. and Hansen, K. (1998)
Analysis of low-dose digital lateral cephalometric radiographs.
Dentomaxillofac Radiol*,* 27: (3): 136-139.

NHS (2003)
"Digest of statistics 2003".
www.nhsbsa.nhs.uk

NHS (2007)
The Ionising Radiation (Medical Exposure) Regulations 2000.
www.legislation.gov.uk

Ongkosuwito, E.M., Katsaros, C., Van 't Hof, M.A. Bodegom, J.C. and Kuijpers-Jagtman, A.M. (2002)
The reproducibility of cephalometric measurements: a comparison of analogue and digital methods.
Eur J Orthod*,* 24: (6): 655-665.

Richardson, A. (1966)
An investigation into the reproducibility of some points, planes, and lines used in cephalometric analysis.
Am J Orthod*,* 52: (9): 637-651.

Richardson, A. (1981)
A comparison of traditional and computerised methods of cephalometric analysis.
Eur J Orthod*,* 3: (1): 15-20.

Rudolph, D.J., Sinclair, P.M. and Coggins, J.M. (1998)
Automatic computerized radiographic identification of cephalometric landmarks.
Am J Orthod Dentofacial Orthop*,* 113: (2): 173-179.

Sayinsu, K., Isik, F., Trakyali, G. and Arun, T. (2007)
An evaluation of the errors in cephalometric measurements on scanned cephalometric images and conventional tracings.
Eur J Orthod*,* 29: (1): 105-108.

Servomaa, A. and Tapiovaara, M. (1998)
Organ Dose Calculation in Medical X Ray Examinations by the Program PCXMC.
Radiation Protection Dosimetry*,* 80: (1-3): 213-219.

Shi, X.Q. and Li, G. (2009)
Detection accuracy of approximal caries by black-and-white and color-coded digital radiographs.
Oral Surg Oral Med Oral Pathol Oral Radiol Endod*,* 107: (3): 433-436.

Shrout, M.K., Russell, C.M., Potter, B.J., Powell, B.J. and Hildebolt, C.F. (1996)
Digital enhancement of radiographs: can it improve caries diagnosis?
J Am Dent Assoc*,* 127: (4): 469-473.

Sikorski, P.A. and Taylor, K.W. (1984)
The effectiveness of the thyroid shield in dental radiology.
Oral Surg Oral Med Oral Pathol*,* 58: (2): 225-236.

Solow, B. and Kreiborg, S. (1988)
A cephalometric unit for research and hospital environments.
Eur J Orthod*,* 10: (4): 346-352.

Solow, B. and Tallgren, A. (1971)
Natural head position in standing subjects.
Acta Odontol Scand*,* 29: (5): 591-607.

Tanimoto, K., Ogawa, M., Kodera, Y., Tomita, S. and Wada, T. (1989)
A filter for use in lateral cephalography.
Oral Surg Oral Med Oral Pathol*,* 68: (5): 666-669.

Taylor, T.S., Ackerman, R.J., Jr. and Hardman, P.K. (1988)
Exposure reduction and image quality in orthodontic radiology: a review of the literature.
Am J Orthod Dentofacial Orthop*,* 93: (1): 68-77.

Thunthy, K.H. and Manson-Hing, L.R. (1978)
Effect of mAs and kVp on resolution and on image contrast.
Oral Surg Oral Med Oral Pathol*,* 46: (3): 454-461.

Turner, P.J. and Weerakone, S. (2001)
An evaluation of the reproducibility of landmark identification using scanned cephalometric images.
J Orthod*,* 28: (3): 221-229.

Tyndall, D.A., Matteson, S.R., Soltmann, R.E., Hamilton, T.L. and Proffit, W.R. (1988)
Exposure reduction in cephalometric radiology: a comprehensive approach.
Am J Orthod Dentofacial Orthop*,* 93: (5): 400-412.

Van Der Stelt, P.F. (2005)
Filmless imaging: the uses of digital radiography in dental practice.
J Am Dent Assoc*,* 136: (10): 1379-1387.

Visser, H., Rodig, T. and Hermann, K.P. (2001)
Dose reduction by direct-digital cephalometric radiography.
Angle Orthod*,* 71: (3): 159-163.

Viteporn, S. (1995)
"The technique of cephalometric radiography."
Orthodontic Cephalometry.
London: Mosby-Wolfe

Wall, B.F., Fisher, E.S., Paynter, R., Hudson, A. and Bird, P.D. (1979)
Doses to patients from pantomographic and conventional dental radiography.
Br J Radiol*,* 52: (621): 727-734.

Watson, W.G. (1982)
Radiation--diffusion or confusion.
Am J Orthod*,* 82: (3): 257-260.

Webber, R.L., Benton, P.A. and Ryge, G. (1968)
Diagnostic variations in radiographs.
Oral Surg Oral Med Oral Pathol*,* 26: (6): 800-809.

Wenzel, A. (1993)
Computer-aided image manipulation of intraoral radiographs to enhance diagnosis in dental practice: a review.
Int Dent J*,* 43: (2): 99-108.

Wenzel, A. (1998)
Digital radiography and caries diagnosis.
Dentomaxillofac Radiol*,* 27: (1): 3-11.

Whaites, E. (2002)
Essentials of Dental Radiography and Radiology.
Elsevier Health Sciences

White, S.C. and Pharoah, M.J. (2004)
Oral radiology : principles and interpretation.
St. Louis Mosby.

APPENDICES

CONSULTANT QUESTIONNAIRE

Dose Optimisation In Contemporary Digital Radiographic Cephalometry

Consultant Questionnaire

Scenario:

You have treatment planned a case from orthodontic records which include intra-oral, extra-oral photos, radiographs and study models.

You subsequently realize that the provided lateral cephalogram may have been traced inaccurately.

The question…

What is the smallest amount of error of the cephalometric measurements listed below that may influence you to change your treatment plan?

Please indicate the amount of error next to each cephalometric measurement in the table below.

Cephalometric Measurement	Amount of error (degree's/mm's)
SNA	
SNB	
ANB	
SN-Maxillary Plane Angle	
MMPA	
Upper incisors-Maxillary plane angle	
Lower Incisors-Mandibular plane angle	
Lower incisors - APo	
Nasolabial Angle	

Any questions please feel free to ask me.

Many thanks for your time in advance.

Rahul Khiroya ( )

IMAGE ANALYSIS INSTRUCTION SHEET

Operator Name	
User Name	OPERATOR__

Instructions for image analysis

1. Enter Dolphin.

2. In the 'Patient Lookup' box type in and then select your username

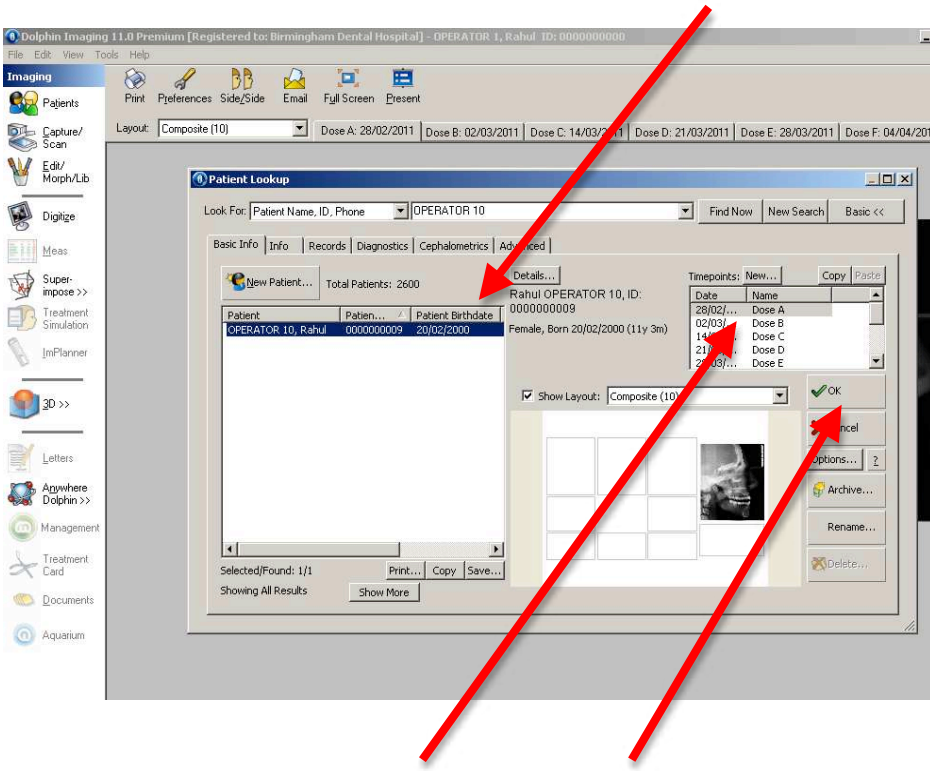

3. Under 'Timepoints' select 'Dose A' and click 'OK'

4. Select 'Digitize' to begin the process of tracing the cephalogram

5. On the ‘digitize setup’ (prior to commencing cephalometric analysis by clicking ‘Start Digitize’):

    a. Under ‘Ceph analyses’ select ‘Rahul MPhil’

    b. Under ‘Auto-drawn structures’ uncheck any blue highlighted structures

    c. Under ‘Calibrate Image’ enter a ‘Ruler Length’ of 40mm

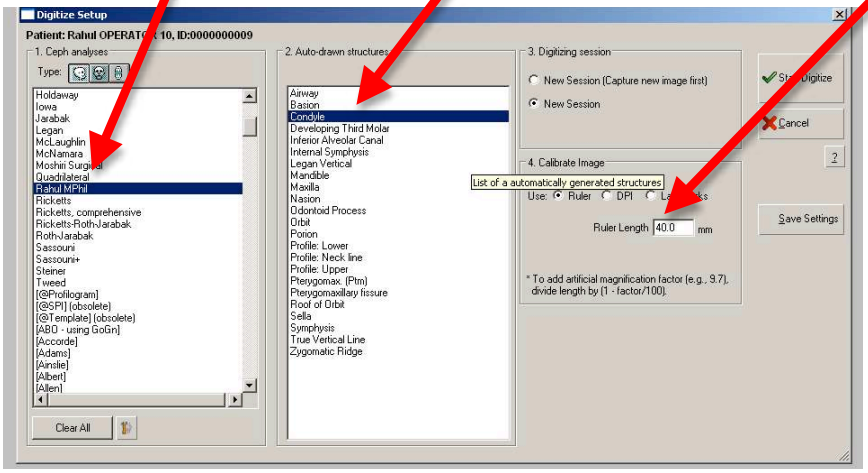

6. As you view and plot the specified landmarks please use the image enhancement features of Dolphin to allow for best possible visual perception of the cephalometric landmarks.

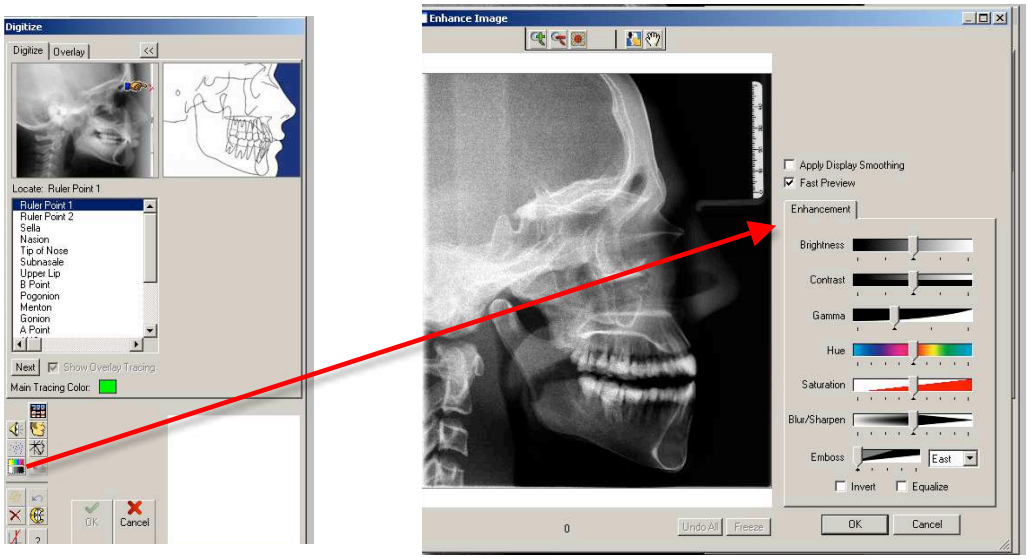

7. Whilst enhancing visualization and plotting landmarks please concurrently fill in the corresponding dated Likert Scale form for the image in question (the instructions are on each form).

8. Once analysis is complete please do not save the enhanced image. This will be offered as an option by the Dolphin software.

Following a respite period of approximately one week please carry out the same but for the cephalogram on Timepoint 'Dose B'. The following is to be done for one image a week until all images up till Timepoint 'Dose I' have been analyzed.

In total with the 9 time-points I would aim to collect the folders of you in 8-9 weeks time.

I would just like to thank you once again for taking part in this research!

CEPHALOMETRIC ANALYSIS RAW DATA

Effective Dose 0.29µSv

Cephalometric Measurement	Operator									
	1	2	3	4	5	6	7	8	9	10
SNA (^{0})	96.9	96.9	96.9	97.8	96.2	95.6	98.1	96.6	96.5	96.8
SNB (^{0})	92.2	92.6	92.6	93.7	93.3	94.4	92.9	92.7	92.8	93
ANB (^{0})	4.7	4.3	4.3	4.2	2.9	1.2	5.2	3.9	3.6	3.9
SN-Maxillary Plane (^{0})	3	-4	-9.7	-1	3.2	2.4	-0.5	-8.6	-6.3	-7.2
Palatal-Mand Angle (^{0})	21.9	28	31.6	25.8	21.6	23.2	28.3	31.1	32.2	30
U1 - Maxillary Plane (^{0})	118.2	112.1	105.9	115.3	118.7	117.6	114.8	106.8	106.9	107.3
IMPA (L1-MP) (^{0})	86.8	84.9	90.5	86.5	88.3	84.4	82	83.9	86.7	85.1
L1 Protrusion (L1-APo) (mm)	4.5	3.9	4.2	4.3	5.2	5.1	5.4	4	4.1	4.4
Nasiolabial Angle (Col-Sn-UL) (^{0})	114.9	103.5	104.3	116.3	113.9	99	115.7	125.9	110.3	115.7

Effective Dose 0.60µSv

Cephalometric Measurement	Operator									
	1	2	3	4	5	6	7	8	9	10
SNA (^{0})	90.3	97	96.6	97.5	97.7	96.2	94.3	96.5	96	96
SNB (^{0})	88.1	92.9	92.3	93.5	93.3	94.6	93.1	92.7	92.6	92.5
ANB (^{0})	2.2	4.1	4.3	4	4.4	1.7	1.3	3.8	3.4	3.6
SN-Maxillary Plane (^{0})	5.6	-9.4	-8.9	-1.3	2.8	3.8	2	-7.9	-8.6	-6.2
Palatal-Mand Angle (^{0})	21.8	32.4	32.3	22.7	23.7	21	22.1	30.6	33	30
U1 - Maxillary Plane (^{0})	116.6	105.1	105	115.2	117.3	117.9	117.5	105.4	105	107.6
IMPA (L1-MP) (^{0})	87.4	89	86.8	85.1	83.9	84.2	88.4	85.9	85.5	84.3
L1 Protrusion (L1-APo) (mm)	4.5	4.6	3.8	4.5	4.8	4.2	7.6	4.4	3.9	4.3
Nasiolabial Angle (Col-Sn-UL) (^{0})	117	113.7	99.3	118.9	112.6	112.7	-82	110.9	104.7	115.7

Effective Dose 0.49µSv

Cephalometric Measurement	Operator									
	1	2	3	4	5	6	7	8	9	10
SNA (^{0})	94.9	97.3	96.7	97.1	96.6	95.9	97.8	97	97.3	95.8
SNB (^{0})	91.5	92.8	91.8	92.8	93.7	94.5	93	92.8	91.9	92.1
ANB (^{0})	3.4	4.4	4.9	4.3	2.9	1.3	4.7	4.3	5.3	3.7
SN-Maxillary Plane (^{0})	3.8	-8.1	-12.5	-7.6	-7.3	2.9	1.9	-7.3	-8.8	-7.4
Palatal-Mand Angle (^{0})	20.8	32.3	36	29.3	32.4	22.5	22.2	29.6	33.3	31.2
U1 - Maxillary Plane (^{0})	116.1	109.5	99.1	105.3	108.4	118.3	114.3	108.9	102.4	106.9
IMPA (L1-MP) (^{0})	86.4	82.8	83.5	85.2	80.4	83.4	82.5	83.9	83.1	84.1
L1 Protrusion (L1-APo) (mm)	4.8	4.7	4.8	4.6	4.6	4.6	4	4.3	3.9	4.6
Nasiolabial Angle (Col-Sn-UL) (^{0})	117.7	111.6	117.8	111.4	115.2	117.6	136.6	112.7	109.8	116.5

Effective Dose 0.38µSv

Cephalometric Measurement	Operator									
	1	2	3	4	5	6	7	8	9	10
SNA (^{0})	95.7	96	96.7	97.3	96.3	96.1	96.7	95.6	96.8	95.6
SNB (^{0})	91.9	92.2	92.3	93	93.6	95	92.9	91.7	92.6	92
ANB (^{0})	3.9	3.8	4.4	4.3	2.7	1.1	3.7	3.8	4.1	3.7
SN-Maxillary Plane (^{0})	2.2	-7.8	-7.3	-5.3	-8.4	0.3	-0.4	-7.4	-7.7	-6.5
Palatal-Mand Angle (^{0})	21.7	33.7	29	28.6	33.9	25.4	26.6	30.1	33.3	30.5
U1 - Maxillary Plane (^{0})	114.5	106.9	108.8	109.3	108	116.5	111.8	108.5	106	108.7
IMPA (L1-MP) (^{0})	83.6	82.7	84.8	83.6	85.3	82	84.2	83.9	84.6	84
L1 Protrusion (L1-APo) (mm)	4.7	5	4.3	4.3	4.7	4.1	6.2	4.4	10.5	4.4
Nasiolabial Angle (Col-Sn-UL) (^{0})	117	115.6	118.7	113.8	116.8	115.6	122	110.9	104.9	114.8

Effective Dose 0.22µSv

Cephalometric Measurement	Operator									
	1	2	3	4	5	6	7	8	9	10
SNA (^{0})	95.7	95.4	95.6	96.8	96.6	95.4	97.4	96.8	96.3	95.4
SNB (^{0})	92.1	91.5	91.7	92.6	93.1	92.9	92.3	92.5	92.4	92.4
ANB (^{0})	3.6	3.9	3.8	4.2	3.5	2.6	5.1	4.3	3.9	3
SN-Maxillary Plane (^{0})	3.5	-7.8	-7.4	-8	-7.6	3.1	-7.9	-8.3	-7.5	-6.8
Palatal-Mand Angle (^{0})	21.4	33.4	31.5	31.9	34.3	22.1	32.7	30.8	31.5	30.6
U1 - Maxillary Plane (^{0})	119.3	107.5	106.5	103	106.8	118.7	101.1	106.3	106.6	109.2
IMPA (L1-MP) (^{0})	83.4	83	82.3	83.1	84.7	84.2	83.6	86.2	84.3	83.7
L1 Protrusion (L1-APo) (mm)	4.5	4.5	4.7	4.4	4.7	4.9	4.4	4.2	4.6	5
Nasiolabial Angle (Col-Sn-UL) (^{0})	120.6	117.6	117.4	111.2	112.5	114.4	139.8	115.3	110.4	118.4

Effective Dose 0.29µSv (REPEAT)

Cephalometric Measurement	Operator									
	1	2	3	4	5	6	7	8	9	10
SNA (^{0})	96.4	96.9	96.8	97.1	96.6	96.1	98.2	96.9	95.9	96.2
SNB (^{0})	92.4	92.1	92.8	92.5	93.9	92.9	93.5	92.6	92.6	92.5
ANB (^{0})	4	4.7	3.9	4.6	2.7	3.2	4.7	4.2	3.3	3.8
SN-Maxillary Plane (^{0})	2.5	-6.1	-9.4	-1.6	-2.1	3	-5.5	-8.7	-7.7	-8.2
Palatal-Mand Angle (^{0})	22	31.5	32.1	25.5	27.2	21.5	30.1	31.5	32.3	31.5
U1 - Maxillary Plane (^{0})	115.4	110.6	106.5	114	112.8	117.5	109.8	104.6	106.1	105.9
IMPA (L1-MP) (^{0})	87.1	85	87.8	82.6	82.3	85.2	87.7	86.2	86	87.3
L1 Protrusion (L1-APo) (mm)	4.5	4.5	4.5	4	4.4	4.6	14.2	4.5	3.5	4.4
Nasiolabial Angle (Col-Sn-UL) (^{0})	133.6	115.8	116.4	121.7	117	119.3	104	113.7	105.7	115

Effective Dose 0.60µSv (REPEAT)

Cephalometric Measurement	Operator									
	1	2	3	4	5	6	7	8	9	10
SNA (^{0})	95.7	95.9	97.3	96.8	96.6	96.4	96.2	96.8	96.9	96
SNB (^{0})	91.9	92.4	92.8	92.8	93.5	93.4	90.9	92.8	92.7	93.3
ANB (^{0})	3.8	3.5	4.5	4	3.1	3	5.3	4	4.2	2.7
SN-Maxillary Plane (^{0})	2.5	-7	-9.2	-1.1	-7.5	2.6	-5.3	-7.7	-7.9	-6.8
Palatal-Mand Angle (^{0})	21.9	29.6	31.4	24.9	33.3	22.8	32.4	30.8	31.3	30.4
U1 - Maxillary Plane (^{0})	114.7	107.3	107.1	113.4	106.3	116.6	108	107.2	106	106.4
IMPA (L1-MP) (^{0})	87	84.5	87.9	83.7	81.8	83	86.7	85	84.9	85.6
L1 Protrusion (L1-APo) (mm)	4.2	4.6	4.7	5	4.5	4.5	4.8	4.3	3.4	4.6
Nasiolabial Angle (Col-Sn-UL) (^{0})	120.4	116.5	122.7	115.1	112.2	110.6	123.9	113	113.9	117.2

Effective Dose 0.13µSv

Cephalometric Measurement	Operator									
	1	2	3	4	5	6	7	8	9	10
SNA (^{0})	96.2	96.9	96	97.3	97.5	96.6	95.1	96.2	96.6	95.9
SNB (^{0})	92.5	92.9	92.2	93	93.8	93.3	90.4	92.2	92.7	92.5
ANB (^{0})	3.7	4	3.8	4.3	3.7	3.3	4.6	4.1	3.8	3.4
SN-Maxillary Plane (^{0})	1.9	-9.4	-8.2	-10	-8.3	2	-4.7	-8.5	-9.5	-7.6
Palatal-Mand Angle (^{0})	23.1	36	31.6	34.2	33.9	23.5	32.5	32.3	34.6	31.8
U1 - Maxillary Plane (^{0})	115.8	109.2	106	100.4	107.9	117.2	106.6	103.7	103.8	106.4
IMPA (L1-MP) (^{0})	82.3	85.1	83.6	81.9	83.2	83.8	82.3	83.7	83.1	85.5
L1 Protrusion (L1-APo) (mm)	4.5	3.7	4.7	4.8	4.6	4.7	5.5	4.7	3.6	4.4
Nasiolabial Angle (Col-Sn-UL) (^{0})	118.7	118.6	115.4	118.4	110.1	116.4	136.9	115.2	106.9	116.5

Effective Dose 0.06µSv

Cephalometric Measurement	Operator									
	1	2	3	4	5	6	7	8	9	10
SNA (^{0})	97.3	98.8	96.7	96.6	96.7	96.3	96.7	97.3	96.3	97.1
SNB (^{0})	93.1	93.9	92.9	92.2	93.3	93.4	92	93.1	92.5	93.7
ANB (^{0})	4.1	4.9	3.8	4.4	3.4	2.8	4.7	4.2	3.8	3.4
SN-Maxillary Plane (^{0})	1.4	-7.9	-8.9	-7.2	-8.2	2.9	-3.9	-9.1	-8.3	-8.3
Palatal-Mand Angle (^{0})	22.5	32.2	30.7	33.1	33.7	21.8	30.8	32.1	33.7	31.4
U1 - Maxillary Plane (^{0})	116.6	110.5	105.6	107.4	109.2	119	109.2	104.6	105.2	107.5
IMPA (L1-MP) (^{0})	85.4	84.2	84.9	85.1	82.6	84.1	80.8	83.3	85.4	84.5
L1 Protrusion (L1-APo) (mm)	4.3	4	4.6	3	4.9	4.3	4.9	4.6	3.9	4.2
Nasiolabial Angle (Col-Sn-UL) (^{0})	121.3	120.3	110.8	116.9	114.9	116	125.3	114.6	110.5	118.4

Landmark visibility grading raw data

Effective Dose 0.29µSv

Cephalometric Landmark	Operator									
	1	2	3	4	5	6	7	8	9	10
Sella	3	3	3	2	3	3	3	3	3	3
Nasion	2	3	3	3	3	3	2	3	3	3
Subnasale	1	3	3	3	3	3	3	2	3	3
Upper lip	1	1	2	3	2	2	1	2	1	2
B Point	3	3	3	3	3	3	3	3	3	3
Pogonion	3	3	3	3	3	3	3	3	3	3
Menton	3	3	3	3	3	3	3	3	3	3
Gonion	3	3	3	3	3	3	3	3	3	3
A Point	3	2	2	3	3	3	2	2	2	3
ANS	3	3	2	2	3	3	1	3	2	2
PNS	2	1	2	2	3	2	1	2	2	1
Lower incisor tip	3	3	3	3	3	3	3	3	3	3
Lower incisor root apex	3	2	2	3	3	3	3	2	2	3
Upper Incisor tip	3	3	3	3	3	3	3	3	3	3
Upper incisor root apex	3	2	2	3	3	2	3	2	2	3

Effective Dose 0.60µSv

Cephalometric Landmark	Operator									
	1	2	3	4	5	6	7	8	9	10
Sella	3	3	3	3	3	3	3	3	3	3
Nasion	2	3	3	3	3	3	2	3	3	3
Subnasale	3	3	2	3	3	3	3	3	3	3
Upper lip	2	1	2	1	2	2	2	1	1	2
B Point	3	3	3	3	3	3	3	3	3	3
Pogonion	3	3	3	3	3	3	3	3	3	3
Menton	3	3	3	3	3	3	3	3	3	3
Gonion	3	3	3	3	3	3	3	3	3	3
A Point	3	3	3	3	3	3	3	3	3	3
ANS	2	3	3	3	3	3	2	3	2	2
PNS	2	2	2	3	3	2	2	2	3	1
Lower incisor tip	3	3	3	3	3	3	3	3	3	3
Lower incisor root apex	2	2	2	3	3	3	3	2	3	3
Upper Incisor tip	3	3	2	3	3	3	3	3	3	3
Upper incisor root apex	2	3	3	3	3	2	3	2	3	3

Effective Dose 0.49µSv

Cephalometric Landmark	Operator									
	1	2	3	4	5	6	7	8	9	10
Sella	3	3	3	3	3	3	3	3	3	3
Nasion	2	3	3	3	3	3	2	3	3	3
Subnasale	3	3	3	3	3	3	3	3	3	3
Upper lip	1	1	1	1	2	2	1	2	1	1
B Point	3	3	3	3	3	3	3	3	3	3
Pogonion	3	3	3	3	3	3	3	3	3	3
Menton	3	3	3	3	3	3	3	3	3	3
Gonion	3	3	3	3	3	3	3	3	3	3
A Point	3	3	3	3	3	3	3	3	3	3
ANS	2	3	3	3	3	3	3	3	3	3
PNS	2	3	2	2	3	2	3	3	3	2
Lower incisor tip	3	3	3	3	3	3	3	3	3	3
Lower incisor root apex	1	2	2	3	2	2	3	1	2	2
Upper Incisor tip	3	3	3	3	3	3	3	3	3	3
Upper incisor root apex	2	2	2	3	3	2	3	2	3	3

Effective Dose 0.38µSv

Cephalometric Landmark	Operator									
	1	2	3	4	5	6	7	8	9	10
Sella	3	3	3	3	3	3	3	3	3	3
Nasion	2	3	3	3	3	3	2	3	3	3
Subnasale	3	3	3	3	3	3	3	3	3	2
Upper lip	2	2	2	2	2	2	2	2	1	1
B Point	3	3	3	3	3	3	3	3	2	3
Pogonion	3	3	3	3	3	3	3	3	3	3
Menton	3	3	3	3	3	3	3	3	3	3
Gonion	3	3	3	3	3	3	3	3	3	3
A Point	3	3	3	3	3	3	3	3	3	3
ANS	3	3	3	3	3	3	3	3	3	3
PNS	2	3	2	2	3	3	3	2	3	1
Lower incisor tip	3	3	3	3	3	3	3	3	3	3
Lower incisor root apex	1	2	2	3	2	3	3	2	3	2
Upper Incisor tip	3	3	3	3	3	3	3	3	3	3
Upper incisor root apex	2	3	2	3	3	3	3	2	3	3

Effective Dose 0.22µSv

Cephalometric Landmark	Operator									
	1	2	3	4	5	6	7	8	9	10
Sella	3	3	3	3	3	3	3	3	3	3
Nasion	3	3	3	3	3	3	3	3	3	3
Subnasale	3	3	3	3	3	3	3	3	3	3
Upper lip	3	3	2	2	2	2	2	2	1	1
B Point	3	3	3	3	3	3	3	3	3	3
Pogonion	3	3	3	3	3	3	3	3	3	3
Menton	3	3	3	3	3	3	3	3	3	3
Gonion	3	3	3	3	3	3	3	3	3	2
A Point	3	3	3	3	3	3	3	3	3	3
ANS	3	3	3	3	3	3	3	3	3	3
PNS	3	3	2	2	3	3	2	2	3	1
Lower incisor tip	3	3	3	3	3	3	3	3	3	3
Lower incisor root apex	2	2	1	3	2	2	3	2	3	1
Upper Incisor tip	3	3	3	3	3	3	3	3	3	3
Upper incisor root apex	2	3	2	3	3	2	3	2	2	3

Effective Dose 0.29µSv (REPEAT)

Cephalometric Landmark	Operator									
	1	2	3	4	5	6	7	8	9	10
Sella	3	3	3	3	3	3	3	3	3	3
Nasion	3	3	3	3	3	3	3	3	3	3
Subnasale	3	3	2	3	3	3	3	3	3	2
Upper lip	2	3	3	3	2	1	1	2	1	2
B Point	3	3	3	3	3	3	3	3	3	3
Pogonion	3	3	3	3	3	3	3	3	3	3
Menton	3	3	3	3	3	3	3	3	3	3
Gonion	2	3	3	3	3	3	3	3	3	3
A Point	3	2	3	3	3	2	3	3	3	3
ANS	2	3	3	3	3	3	3	3	3	2
PNS	3	3	3	3	3	3	2	2	3	1
Lower incisor tip	3	3	3	3	3	3	3	3	3	3
Lower incisor root apex	3	2	2	3	3	2	3	2	2	2
Upper Incisor tip	3	3	3	3	3	3	3	3	3	3
Upper incisor root apex	2	2	2	3	3	2	3	2	2	3

Effective Dose 0.60µSv (REPEAT)

Cephalometric Landmark	Operator									
	1	2	3	4	5	6	7	8	9	10
Sella	3	3	3	3	3	3	3	3	3	3
Nasion	3	3	3	3	3	3	3	3	3	3
Subnasale	3	3	3	3	3	3	3	3	3	2
Upper lip	3	3	1	3	3	1	1	2	1	1
B Point	3	3	3	3	3	3	3	3	3	2
Pogonion	3	3	3	3	3	3	3	3	3	3
Menton	3	3	3	3	3	3	3	3	3	3
Gonion	3	3	3	3	3	3	3	3	3	3
A Point	3	3	3	3	3	3	3	3	3	3
ANS	2	3	3	3	3	2	3	3	3	3
PNS	3	3	2	2	3	3	3	2	3	1
Lower incisor tip	3	3	3	3	3	3	3	3	3	3
Lower incisor root apex	3	3	2	3	3	2	3	2	2	2
Upper Incisor tip	3	3	3	3	3	3	3	3	3	3
Upper incisor root apex	2	3	2	3	3	3	3	2	2	3

Effective Dose 0.13µSv

Cephalometric Landmark	Operator									
	1	2	3	4	5	6	7	8	9	10
Sella	3	1	3	3	3	3	3	3	3	3
Nasion	3	1	3	3	3	3	3	3	3	3
Subnasale	3	1	3	3	3	3	3	3	3	2
Upper lip	3	1	2	3	3	1	2	2	1	2
B Point	3	1	3	3	3	3	3	3	3	2
Pogonion	3	1	3	3	3	3	3	3	3	3
Menton	3	1	3	3	3	3	3	3	3	3
Gonion	3	1	3	3	3	3	3	3	3	3
A Point	3	1	3	3	3	3	2	2	3	2
ANS	2	1	3	3	3	3	2	3	3	3
PNS	3	1	2	2	3	3	2	2	3	1
Lower incisor tip	3	1	3	3	3	3	3	3	3	3
Lower incisor root apex	2	2	2	2	3	2	2	2	3	1
Upper Incisor tip	3	1	3	3	3	3	3	3	3	3
Upper incisor root apex	2	1	1	3	3	2	3	2	2	2

Effective Dose 0.06µSv

Cephalometric Landmark	Operator									
	1	2	3	4	5	6	7	8	9	10
Sella	3	3	2	3	3	3	2	2	3	2
Nasion	3	3	3	3	3	3	2	3	3	3
Subnasale	3	3	2	3	3	3	3	2	3	3
Upper lip	2	3	1	3	2	1	2	1	1	1
B Point	3	3	3	3	3	3	3	3	3	2
Pogonion	3	3	3	3	3	3	3	3	3	3
Menton	3	3	3	3	3	3	3	3	3	3
Gonion	3	3	3	3	3	3	3	2	3	2
A Point	3	3	3	3	3	3	3	2	3	2
ANS	3	3	3	3	3	3	2	3	3	3
PNS	2	3	1	2	3	3	2	2	2	1
Lower incisor tip	3	3	3	3	3	3	3	3	3	3
Lower incisor root apex	1	2	1	2	3	2	2	1	2	1
Upper Incisor tip	3	3	3	3	3	3	3	3	3	3
Upper incisor root apex	1	3	2	3	3	2	3	1	2	1

HOSPITAL SURVEY QUESTIONNAIRE

LATERAL CEPHALOMETRY QUESTIONNAIRE

Date:
Completed By:
Trust:
Hospital/Clinic:
Department:
Room:

X-ray Equipment

Equipment Make & Model:

Imaging Modality

Integrated Digital Detector **Yes/No** (delete as appropriate)

Computed Radiography **Yes/No** (delete as appropriate)

If yes…..

Make + Model CR Reader?	
Make and Model Imaging Plates?	

Film/Screen **Yes/No** (delete as appropriate)

If yes…..

Film Make and Type?	
Film Speed?	
Intensifying screen make and type?	

Lateral Cephalometry Exposure Settings

	Child (7-12years)	***Small Adult (15years)***
kV:		
mA:		
Time (s):		

HOSPITAL SURVEY RAW DATA

Hospital	X-ray Equipment	Imaging Modality		Small Adult (15 years)				
		CR Reader	Imaging Plates	kV	mAs	E	Salivary	Thyroid
						(µSv)	(µGy)	(µGy)
5	Gendex Orthoralix 9200	Agfa ADC Solo	Agfa	78	4.8	0.9	27.2	2.5
8*	Sirona Orthophos XG5			69	139.5	0.6	18.1	1.5
9	Instrumentarium Orthoceph OC20(	Kodak Direct View CR975	Kodak	66	141.2	0.6	16.8	1.4
7	Instrumentarium Orthoceph OC10(	Kodak Direct View CR850	Kodak PQ	73	3.84	0.7	19.1	1.8
2	Instrumentarium Orthoceph OC10(	Konica Regius 170	Konica Regius RP35	77	7.68	1.4	39.3	3.6
1	Kodak 8000C			78	12	2.4	68.0	6.2
4	Planmeca PM2002	Agfa ADC Solo	Agfa ADCCHR	72	6	1.0	29.0	2.7
10	Instrumentarium Orthoceph OC10(	Kodak Direct View CR975	Kodak	77	2.76	0.5	15.2	1.4
6	Gendex Orthoralix 5000	Philips PCR Eleva	Philips	78	4.8	0.9	27.2	2.5
3	Sirona Orthophos	Agfa	Agfa	79	6.3	1.4	39.3	3.6

** Integrated Digital Detector*